Chapter 2
Estimation of Net Primary Productivity: An Introduction to Different Approaches

Pramit Kumar Deb Burman

Abstract The net primary productivity (*NPP*) is defined as the net carbon gain by plants in natural and agricultural ecosystems, which is computed by subtracting the autotrophic respiration from the gross photosynthetic carbon uptake by the ecosystems. It acts as the indicators of carbon sequestration, ecosystem health, and agricultural yield which are important in the context of climate change, its impact and mitigation, and food security. The *NPP* can be estimated in multiple ways including the direct and indirect measurements and modelling. The various direct *NPP* measurements are ground-based in situ observations of ecosystem-atmosphere carbon flux such as the micrometeorological flux-gradient method, eddy covariance, flux chamber measurements etc. The indirect measurements of *NPP* include the satellite-derived *NPP* estimates which are computed from the directly measured spectral reflectances, using different biophysical relations such as the light use efficiency model etc. However the accuracy of these products varies geospatially and largely depends on the retrieval of input parameters and representativeness of underlying model parameterization. There are two major modelling approaches to estimate the *NPP* namely bottom-up and top-down estimates. The bottom-up models compute the *NPP* from the directly recorded variables such as temperature, precipitation, radiation, wind, atmospheric CO_2 concentration etc. using the biome-specific functional relations due to which these are also known as the process-based models. The top-down or inverse models use the matrix inversion method to predict the sources and sinks of CO_2 emission in a region from the directly measured concentrations by the surface stations and/or satellites and thus the *NPP* of that region. The *NPP* estimates from measurements and models are used to calculate the carbon budgets at different scales from ecosystem-level to global scale. However significant

P. K. Deb Burman (✉)
Centre for Climate Change Research, Indian Institute of Tropical Meteorology,
Ministry of Earth Sciences, Pune 411008, India
e-mail: pramit.cat@tropmet.res.in; pkdebburman@gmail.com

Department of Atmospheric and Space Sciences, Savitribai Phule Pune University, Pune 411007, India

uncertainties exist in such estimates due to insufficient surface measurements, under-representation of several regions and ecosystems, imperfect boundary conditions and parameterizations in models. While the direct measurements provide more accurate estimates of *NPP*, these require to be carried over for long duration using multiple different instruments which are prone to errors and data-loss whereas the models can provide large-scale estimates of *NPP* but need to be validated against realistic in situ measurements across an wide array of ecosystems. The aforementioned aspects of *NPP* estimation are discussed in detail in the present chapter.

Keywords Carbon cycle · Terrestrial ecosystems · Gross primary productivity · Net ecosystem productivity · Eddy covariance · Ecosystem models · Inverse models · Vegetation indices

2.1 Introduction

Since the industrial revolution the atmospheric CO_2 concentration (c_a in ppm) has risen from ~280 to 416 ppm (till the time of writing this book chapter) in an unprecedented rate (https://www.esrl.noaa.gov/gmd/ccgg/trends/mlo.html). Due to the increased energy demand the carbon stored in fossil fuel deposits has been burnt and released into the atmosphere. To meet the food and fibre demands of an increasing population the rapid agricultural expansion has taken place at the cost of natural ecosystems such as forests. The increased amount of atmospheric greenhouse gases of which CO_2 is a major component, is changing the Earth's radiation feedback resulting in global warming and paving the way for climate change (IPCC 2013).

Such climate change is predicted to have adverse effects on the Earth such as abrupt changes in atmospheric and oceanic circulation patterns, polar ice cap melt, sea-level rise, shifting treeline, increased frequency and intensity of extreme events etc. In order to devise the climate change mitigation strategies the sources and sinks of atmospheric CO_2 need to be identified and their strengths and patterns need to be characterised. The terrestrial ecosystems play a regulatory role in the Earth's radiation budget due to their roles in determining the surface albedo and photosynthetic carbon uptake (Betts 2000). According to the global carbon budget 2019 (Friedlingstein et al. 2019) the terrestrial ecosystems were the largest sink of atmospheric CO_2 in the latest decade during 2009–2018 with a sink-strength of 3.2 ± 0.6 GtC y^{-1}. Several land-based mitigation strategies are designed based on these ecosystems such as afforestation and reforestation, biochar, bioenergy with carbon capture and storage etc. (Minx et al. 2018). Moreover proper quantification of the carbon cycles of these ecosystems is important to estimate the intended nationally determined contribution (INDC) of the nations in compliance with the Paris climate accord.

The changes in c_a, trends of air temperature and precipitation due to climate change will modify the capacity and pattern of the photosynthetic carbon uptake by terrestrial ecosystems (IPCC 2019). The response of the ecosystems to such changes remains uncertain which is required for the climate change impact assessment. For

this purpose the long-term observations of terrestrial carbon cycle are required. It is predicted that in changed environmental conditions the indigenous plant species are at high risk to be replaced by the more sturdy invasive species, thus resulting in the extinction of species and loss of biodiversity (Bongaarts 2019). The accelerated c_a is also predicted to cause forest dieback in several regions (Cox et al. 2004).

In this contest, the present chapter is aimed at the estimation of net primary productivity (*NPP*), a component of the carbon cycle and its significance. The different observation and modelling techniques to achieve this are discussed in the subsequent sections. In compliance with the theme of this book, the contents of this chapter are restricted to the forest ecosystems. It is to be noted that *NPP* estimation of aquatic ecosystems such as marine phytoplankton is a different topic and not discussed here. Also the agricultural ecosystems are not included as those are not considered as natural ecosystems. Considering the wide span of the subject matter and a vast amount of literature existing on the different aspects of the same, I have not tried to make this chapter as a comprehensive review article but as an indicative document on the progress done in this field and its present status. The future directions from here are also discussed briefly towards the end. This topic being an interdisciplinary one, care has been taken in the formulation of the chapter to make it apprehensible to the potential readers who belong to different academic and professional backgrounds.

2.2 Data and Modelling

2.2.1 The Carbon Cycle Components

The flux of any variable is defined as the amount of that variable exchanged across a unit surface per unit time. In this regard the vertical CO_2 flux (F_c) between the ecosystem and atmosphere is the measure of carbon exchanged between the ecosystem and atmosphere, also known as the net ecosystem exchange (*NEE*). It is a resultant of the photosynthetic uptake and respirative loss of carbon which are defined as the gross primary productivity (*GPP*) and total ecosystem respiration (*TER*) respectively. The *TER* is comprised of respired carbon fluxes by the autotrophs and heterotrophs which are defined as autotrophic respiration (R_A) and heterotrophic respiration (R_H) respectively. As per the meteorological convention the negative and positive values of *NEE* stand for the carbon gain and loss by the canopy, which is opposite to the convention followed in ecology. The net ecosystem productivity (*NEP*) is defined as the negative of *NEE*. According to these definitions (Chapin et al. 2006),

$$GPP = NPP + R_A \tag{2.1}$$

$$NPP = NEE + R_H \tag{2.2}$$

and,

$$TER = R_A + R_H \tag{2.3}$$

All the variables used this book chapter are described in Table 2.1.

2.2.2 In Situ Measurements

The *NEE* can be directly estimated from the observations in contrast with *GPP* and *TER*. Hence the *GPP* and *TER* are estimated from the *NEE* measurements using a set of ecophysiological relations among the ecosystem and environmental variables. Following are the different methodologies for measuring *NEE*.

2.2.2.1 Eddy Covariance Measurements

The eddy covariance (EC) method is probably the most accurate technique for estimating the biosphere–atmosphere scalar and energy fluxes using the direct measurements of wind parameters and scalars. It has been widely used across the globe for continuous monitoring of long-term CO_2 exchange by the ecosystems in different geographical location, altitudes and terrains (Baldocchi 2003; Deb Burman et al. 2020a, b). Several continental, regional and national networks exist comprising the dense arrays of such towers (Baldocchi et al. 2001; Beringer et al. 2016; Deb Burman et al. 2017; Deb Burman et al. 2018; Rebmann et al. 2018). A comprehensive global map of such active and past EC flux towers can be found in Burba (2019).

Any variable in the atmosphere is exchanged and mixed among the layers by the random turbulent wind motions, also known as the eddies. In EC method these eddies of different temporal scales are sampled by the fast (5, 10 or 20 Hz) measurements of wind velocity components and gas concentrations. Finally the contributions of all such eddies are summed up to compute the net fluxes using the Reynolds averaging technique (Reynolds 1895; Deb Burman et al. 2018). The ecosystem-atmosphere CO_2 flux (F_c in µmol m^{-2} s^{-1}) is computed from the vertical component of wind velocity (w in m s^{-1}) and atmospheric CO_2 molar concentration (c in µmol m^{-3}) which can be expressed as follows,

$$F_c = \overline{w'c'} \tag{2.4}$$

and

$$X' = X - \overline{X} \tag{2.5}$$

Table 2.1 Variables used in the present study, listed alphabetically

Symbol	Definition	Unit	Reference
A_n	Net CO_2 uptake by leaves	$\mu mol\ m^{-2}\ s^{-1}$	Collatz et al. (1991)
$APAR$	Absorbed Photosynthetically Active Radiation	$W\ m^{-2}$	Running et al. (1999)
α_{nir}	Surface reflectance in the near-infrared range of electromagnetic spectrum	–	Carlson and Ripley (1997)
α_{vis}	Surface reflectance in the visible range of electromagnetic spectrum	–	Carlson and Ripley (1997)
b	Regression parameter	$m\ s^{-1}$	Collatz, et al. (1991)
B	Bowen ratio	–	Stull (1988)
β	Proportionality constant	–	Businger and Oncley (1990)
c	Atmospheric CO_2 molar concentration	$\mu mol\ m^{-3}$	–
$c(z)$	c measured at height z	$\mu mol\ m^{-3}$	–
c_a	Atmospheric CO_2 concentration	ppm	–
c_s	CO_2 concentration at leaf surface	ppm	Collatz et al. (1991)
c_u	Updraft CO_2 molar concentration	$\mu mol\ m^{-3}$	Businger and Oncley (1990)
c_d	Downdraft CO_2 molar concentration	$\mu mol\ m^{-3}$	Businger and Oncley (1990)
EVI	Enhanced vegetation index	–	Jiang et al. (2008)
ε	Actual light use efficiency	$gC\ MJ^{-1}$	Monteith (1972)
ε_F	ε analogous factor for SIF		Guanter et al. (2014)
ε_{max}	Theoretically maximum light use efficiency	$gC\ MJ^{-1}$	Monteith (1972)
f	Ratio of ε_{max} and ε	–	Monteith (1972)
$fAPAR$	Fraction of Absorbed Photosynthetically Active Radiation	–	Running et al. (1999)
F_c	Vertical CO_2 flux	$\mu mol\ m^{-2}\ s^{-1}$	Aubinet et al. (2012)
F_q	Vertical water vapour flux	$mmol\ m^{-2}\ s^{-1}$	Stull (1988)
F_s	Storage flux of CO_2	$\mu mol\ m^{-2}\ s^{-1}$	Aubinet et al. (2012)
GPP	Gross Primary Productivity	$gC\ m^{-2}\ y^{-1}$	Chapin et al. (2006)
h	Measurement height	m	Chapin et al. (2006)
h_s	Relative humidity at leaf surface	–	Collatz et al. (1991)

Table 2.1 (continued)

Symbol	Definition	Unit	Reference
H	Sensible heat flux	$W\ m^{-2}$	Stull (1988)
K_c	Eddy diffusivity factor for CO_2	$m^2\ s^{-1}$	Lee (2018)
K_q	Eddy diffusivity factor for water vapour	$m^2\ s^{-1}$	Lee (2018)
LAI	Leaf Area Index	–	Watson (1947)
LE	Latent heat flux	$W\ m^{-2}$	Stull (1988)
λ	Measurement wavelength	nm	–
m	Regression parameter	–	Collatz et al. (1991)
$NDVI$	Normalized Difference Vegetation Index	–	Carlson and Ripley (1997)
NEE	Net Ecosystem Exchange	$\mu mol\ m^{-2}\ s^{-1}$	Chapin et al. (2006)
NEP	Net Ecosystem Productivity	$gC\ m^{-2}\ y^{-1}$	Chapin et al. (2006)
NPP	Net Primary Productivity	$gC\ m^{-2}\ y^{-1}$	Chapin et al. (2006)
PAR	Photosynthetically Active Radiation	$W\ m^{-2}$	Alados et al. (1996)
q	Atmospheric water vapour molar concentration	$mmol\ m^{-3}$	–
R_A	Autotrophic Respiration	$\mu mol\ m^{-2}\ s^{-1}$	Chapin et al. (2006)
R_H	Heterotrophic Respiration	$\mu mol\ m^{-2}\ s^{-1}$	Chapin et al. (2006)
$r_{a,c}$	Aerodynamic resistance to CO_2 transfer	$m^{-1}\ s$	Lee (2018)
r_b	Leaf boundary layer resistance	$m^{-1}\ s$	Lee (2018)
r_c	Canopy resistance	$m^{-1}\ s$	Lee (2018)
r_s	Stomatal resistance	$m^{-1}\ s$	Lee (2018)
$SAVI$	Soil-Adjusted Vegetation Index	–	Huete (1988)
SIF	Solar-Induced Fluorescence	$W\ m^{-2}\ sr^{-1}\ \mu m^{-1}$	Meroni et al. (2009)
σ_w	Standard deviation of the vertical component of wind velocity	$m\ s^{-1}$	–
TER	Total Ecosystem Respiration	$gC\ m^{-2}\ y^{-1}$	Reichstein (2005)
u^*	Friction velocity	$m\ s^{-1}$	Foken (2008)
VI	Vegetation Index	–	Huete et al. (2002)
VPD	Vapour Pressure Deficit	hPa	–
w	Vertical component of wind velocity	$m\ s^{-1}$	–

Table 2.1 (continued)

Symbol	Definition	Unit	Reference
LSWI	Land-Surface Water Index	–	Fensholt and Sandholt (2003)

where X' stands for the instantaneous fluctuations in the measured values of variable X from its mean over the averaging period ($\overline{X}$). The overbar denotes the temporal averaging which is usually done every 30 or 60 min.

A typical EC measurement setup for CO_2 includes sonic anemometer and infrared gas analyser for wind velocity and CO_2 concentration measurements respectively, which are usually placed at a single height above the ecosystem canopy or at several recommended heights within the canopy (Deb Burman et al. 2019). These measurement heights determine the footprint or representativeness of the EC measurement (Kormann and Meixner 2001; Kljun et al. 2015). In addition the EC tower is instrumented at various levels and depths with a set of associated meteorological, radiation and soil sensors (Aubinet et al. 2012). The fast measurements by EC sensors are prone to various errors such as the random spikes, faulty measurement values due to inaccurate sensor geometry, density fluctuation of the ambient air due to the presence of moisture, obstruction of the wind by the sensors etc. The raw EC data is rigorously filtered for removing such errors following a set of recommended pre-processing techniques such as despiking (Vickers and Mahrt 1997; Mauder et al. 2013), detrending, coordinate rotations (Kaimal and Finnigan 1994), angle of attack correction (Kaimal and Finnigan 1994), Webb-Pearman-Leuning correction (Mauder et al. 2013), low (Moncrieff et al. 1997) and high-pass noise filtering (Moncrieff et al. 2004), time-lag between velocity and concentration measurements (Burba 2013) etc. Such a flux tower is shown in Fig. 2.1 which is installed at the Pichavaram mangrove ecosystem as part of the MetFlux India network in Tamil Nadu, India (Deb Burman et al., 2017; Gnanamoorthy et al. 2019; Chakraborty et al. 2020; Gnanamoorthy et al. 2020).

While implementing these corrections the resulting half-hourly NEE values are flagged according to a 10-point scale from 0 to 9 with increasing order suggesting reduced confidence (Foken et al. 2004). Such classification takes into account the atmospheric conditions including non-stationary and non-integral turbulences. The choice of best quality data depends on the requirement. Usually for developing the functional relationships between carbon flux and environment, the data values not exceeding flag 2 are used while in some cases such strict quality-control results in 60–65% of data loss, mostly during nighttime rendering the remaining data heavily biased towards daytime. In such cases the flags are gradually relaxed for more uniform representation of day and nighttime values in the final data record. The friction velocity (u^*) is a measure of the atmospheric turbulence (Foken 2008). At very low values of turbulence the fundamental principles of EC measurement are violated. To avoid this condition u^*-filtering is done in which the *NEE* values corresponding to u^* below a certain threshold are rejected. This u^*-threshold determination is crucial for the accurate estimation of *NEE* and several recipes exists to determine this

Fig. 2.1 A surface flux tower instrumented at multiple levels with eddy covariance and other associated measurement sensors at the Pichavaram mangroves, Tamil Nadu, India; this tower is part of the MetFlux India network

(Gu et al. 2005; Barr et al. 2013); Wutzler et al. 2018) . Apart from these a certain amount of CO_2 is trapped in the canopy that does not mix with the atmosphere by turbulent mixing. This is termed as the storage flux (Baldocchi 2003). The storage flux between ground and measurement height h (F_s) is computed from the measured CO_2 concentration (c) time series at height h as follows,

$$F_s = \int_0^h \frac{\partial c}{\partial t} dz \qquad (2.6)$$

Finally the *NEE* is computed as ($F_c + F_s$). All of these measures are documented in several books such as Burba and Anderson (2007) and Aubinet et al. (2012). The various quality-control measures result gaps in the data. Gaps also occur due to the instrument malfunctioning at several times. However to account for the NEP of any ecosystem, continuous measurement record is required which is achieved by filling the gaps in data. Several recipes of gap-filling exist in literature e.g. mean diurnal variation (MDV), marginal distribution sampling (MDS), look-up table (LUT) etc. (Moffat et al. 2007; Reichstein 2005). Selection of any particular recipe for gap-filling depends on various factors such as the extent and severity of data loss, environmental conditions, local climatology, availability of supporting measurements etc. These recipes have evolved over years owing to active research by several groups and are documented elsewhere (Falge et al. 2001).

Although the EC measurement offers an unprecedented advantage of real time monitoring of *NEP* of any ecosystem it has its own limitations (Massman and Lee 2002). Advective fluxes remain difficult to be separated from the vertical exchange (Paw et al. 2000; Etzold et al. 2010). The fluxes measured over mountainous, undulated terrains are laced with lots of measurement uncertainty (Geissbühler and Siegwolf 2000). During low-turbulence conditions, mostly in the nocturnal periods fluxes are severely undermined (Aubinet et al. 2010). The EC method is still under active research and evolving fast. A large number of scientific publications and references exist on this technique, its development and adaptations not all of which are possible to be included in the limited span of the present chapter. Interested readers however are suggested to read several such articles appearing in the meteorology, forestry and agricultural journals.

2.2.2.2 Gradient Flux Measurements

In the absence of direct EC measurements F_c can be estimated from the spatial gradient of mean CO_2 molar concentration ($\bar{c}$ in μmol m^{-3}) assuming a diffusive model. In this model $\bar{c}$ is assumed to vary slowly and the Reynolds averaged covariance F_c is parameterized as the function of vertical gradient of $\bar{c}$ as follows,

$$F_c = -K_c \frac{\partial \bar{c}}{\partial z} \qquad (2.7)$$

where, K_c is defined as the eddy diffusivity factor for carbon dioxide. It has the unit of m^2 s^{-1}. Due to the turbulent diffusion CO_2 is transported from high concentration zone to low concentration zone. Hence the negative sign is introduced in Eq. (2.7) to maintain conformity with the flux convention described earlier. In a simplistic setup with two-level measurements Eq. (2.7) can be reformulated as,

$$F_c = -K_c \frac{\overline{c(2)} - \overline{c(1)}}{z(2) - z(1)} \tag{2.8}$$

where, $\overline{c(1)}$ and $\overline{c(2)}$ stand for the mean CO_2 concentrations at lower ($z(1)$) and upper ($z(2)$) measurement heights respectively (Lee 2018).

Although convenient in the absence of fast measurements, the gradient flux measurement technique is heavily criticised for several reasons. In the gradient flux formulation the spatial heterogeneity of CO_2 source strength at the horizontal surfaces of concentration measurement is not considered. Moreover the vertical variation in CO_2 source strength is overlooked (Dyer 1974). This problem is partially circumvented by introducing more concentration measurements in the intermediate levels and fitting a vertical profile to the measured values for computing the gradient. K_c has a strong functional dependency on atmospheric stability for which a set of empirically determined stability correction factors are introduced for better estimation of F_c (Dyer and Hicks 1970; Businger et al. 1971). In practical applications the gradient flux method is mostly used in conjunction with the primary EC measurement with iterative determination of K_c from the latter set of measurements.

2.2.2.3 Resistance Methods

Assuming a constant flux layer, where F_c does not vary with height, Eq. (2.7) can be reformulated as,

$$\overline{c} = -F_c \int_0^h \frac{1}{K_c} dz \tag{2.9}$$

or,

$$F_c = -\overline{c}\frac{1}{\overline{r_{a,c}}} \tag{2.10}$$

where,

$$r_{a,c} = \int_{0}^{h} \frac{1}{K_c} dz \tag{2.11}$$

is defined as the aerodynamic resistance to CO_2 transfer, in analogy to the electrical resistance as defined in the Ohm's law (Lee 2018). The $r_{a,c}$ increases with increasing stability and depth of the diffusion layer. Increased turbulence in the atmosphere decreases $r_{a,c}$.

In addition to aerodynamic resistance, the plant-atmosphere photosynthetic CO_2 exchange pathway involves leaf boundary layer and stomatal resistances, connected in series as the CO_2 molecules transport through these sequentially. The layer of atmosphere in close vicinity of the leaves is usually thin but unperturbed. The exchange of CO_2 through this layer only takes place through molecular diffusion which gives rise to the leaf boundary layer resistance (r_b).

The stomatal resistance (r_s in s m^{-1}) is defined as the resistance faced by CO_2 molecules while escaping to the atmosphere from the stomatal cavity. The plant-atmosphere CO_2 and water vapour exchanges by photosynthesis and transpiration respectively, are coupled by the stomatal opening and closure mechanism (Farquhar and Sharkey 1982). There are two major schemes to parameterize r_s. According to the Jarvis-Stewart formulation (Jarvis 1976; Stewart 1988), r_s is empirically determined from radiation, leaf temperature, vapour pressure deficit (*VPD*) and soil moisture content.

In another approach, introduced by Ball et al. (1987) and Collatz et al. (1991) r_s is expressed as a function of net CO_2 uptake (A_n) and relative humidity and CO_2 concentration at the leaf surface (h_s and c_s, respectively) as follows,

$$r_s = \frac{1}{m \frac{A_n \cdot h_s}{cs} + b} \tag{2.12}$$

where, m and b are the linear regression parameters derived experimentally. These models have been widely used by several researchers and adopted according to different climate types (Leuning 1990; Tuzet et al. 2003; Whitley et al. 2008; Ye and Yu 2008). The inverse of any resistance parameter is defined as the corresponding conductance. In simplified bigleaf models where the entire ecosystem is considered to behave like a single leaf (Monteith et al. 1965), the canopy resistance (r_c) is used to compute the ecosystem-atmosphere fluxes. However, the interpretation of r_c is not trivial. In a simplistic formulation where all the leaves in the canopy can be considered as individual resistors with stomatal resistance r_s connected in parallel, r_c can be expressed as r_c/n where n is the number of leaves in the canopy.

2.2.2.4 Modified Bowen Ratio Method

The Bowen ratio (B) is defined as the ratio of sensible (H in W m^{-2}) and latent (LE in W m^{-2}) heat fluxes. It has been widely used to estimate LE from the energy flux measurements in the absence of water vapour measurement assuming a perfect closure of the surface energy budget known as the Bowen ratio method (Stull 1988). This technique is modified to estimate F_c from the vertical flux of water vapour (F_q in mmol m^{-2} s^{-1}) in the absence of fast measurement of c from the two level slow measurements of $\overline{q}$ and $\overline{c}$ as follows,

$$F_c = \frac{\overline{c(2)} - \overline{c(1)}}{\overline{q(2)} - \overline{q(1)}} \cdot F_q \tag{2.13}$$

where, $\overline{c(1)}$ and $\overline{q(1)}$ are the values of c and atmospheric water vapour molar concentration (q in mmol m^{-3}) at lower measurement height (z1) and $\overline{c(2)}$ and $\overline{q(2)}$ are the values of c and q at upper measurement height (z2). This technique assumes the eddy diffusivities of CO_2 and water vapour transport (i.e. K_c and K_q, respectively) are equal to each other and is known as the modified Bowen ratio method (Meyers et al. 1996).

2.2.2.5 Associated Micro-meteorological Methods

There have been several micrometeorological methods proposed to measure F_c in the absence of fast EC measurements, using the available slow gas concentration measurements as described below.

Disjunct Eddy Covariance

The disjunct eddy covariance (DEA) is a modification of EC method first proposed by Rinne et al. (2001) for measuring the fluxes of volatile organic compounds (VOC). In this method the turbulence is assumed to be fully developed and hence the time series of w and gas concentration are sampled at a much coarser temporal scale than EC method. This method has been used by few researchers to estimate F_c as well with good confidence (Hörtnagl et al. 2010; Baghi et al. 2012).

Eddy Accumulation

The eddy accumulation (EA) method is a modified version of the EC method where air samples are stored in two separate containers based on updraft and downdraft (Hicks and McMillen 1984). The collection time is proportional to the strength of updraft or downdraft i.e. the magnitude of w. After the data is collected for 30 or

60 min the average CO_2 concentration in both the collection volumes is measured and subtracted from each other for computing F_c (the detailed mathematical formulation is similar to the EC method). Instead of sampling all the eddies separately as done in the EC method (within the practically limiting smallest and largest time scales, as decided by the sampling frequency and averaging time), in EA method all the eddies are augmented according to upward or downward motions and the mean concentration for both of these segments are computed. This method was first proposed by Desjardins (1972).

Relaxed Eddy Accumulation

The relaxed eddy accumulation (REA) is a modification of the EA technique where the air volumes are sampled separately at constant flow rate for updrafts and downdrafts, with the separate measurements of CO_2 concentrations for both the volumes. Finally the difference between updraft and downdraft averages of CO_2 molar concentrations ($\overline{c_u}$ and $\overline{c_d}$ respectively) is multiplied by the standard deviation of vertical velocity (σ_w) during the entire duration of updraft or downdraft event and an empirically determined dimensionless factor of proportionality (β) to compute F_c as follows,

$$F_c = \beta \cdot \sigma_w \cdot (\overline{c_u} - \overline{c_d}) \tag{2.14}$$

This method had been first proposed by Businger and Oncley (1990) who also proposed the value of β to be 0.6. However the choice of β is a major source of uncertainty of this method which was later shown to vary within 0.40–0.63 under different experimental conditions by several researchers (Baker et al. 1992; Milne et al. 1999). Additionally the accurate segregation of air samples in updraft and downdraft periods and precise measurement of $\overline{c_u}$ and $\overline{c_d}$ are essential which are difficult to be achieved in field conditions (Pattey et al. 1993). The REA has been mostly used in the measurements of trace gas, aerosol, VOCs and isotopic fluxes (Guenther et al. 1996; Valentini et al. 1997; Myles et al. 2007) for which fast concentration measurements are not available, as required by the EC technique. However, several inter comparison studies have shown the REA to perform well in estimating F_c under strict measurement control as compared to EC method in agricultural and forest ecosystems (Pattey et al. 1993; Gaman et al. 2004). There have been several modifications of REA since its inception such as the hyperbolic relaxed eddy accumulation (HREA) by Bowling et al. (1999) etc. which I am not going to discuss in detail in the limited span of the present chapter. The interested readers are suggested to read the relevant literature for the detailed information on these techniques.

Chamber-Based Measurements

In the chamber-based methods enclosure chambers are used to isolate a part of the atmosphere within which the CO_2 concentration is allowed to change only by the respiration or photosynthesis by the plant, part of plant or soil enclosed by these chambers. The F_c is computed from the change in c over the sampling time interval. The walls of the chambers are impermeable and do not allow the CO_2 inside to interact with the ambient atmosphere through diffusion. In static chamber methods the ambient air flow is restricted (Wang et al. 2010) whereas in dynamic chamber methods the ambient air is allowed to flow through the chamber at a constant base flow rate (Ohkubo et al. 2007). Several different geometries of the chambers exist (Kutsch et al. 2010).

The operation of flux chambers can be manual or automatic. These are portable and have less stringent requirements than the EC technique. However they significantly alter the microclimate within the chamber volume e.g. the opaque chambers increase the probability of dark respiration, static chambers hinder the turbulent mixing etc. Despite the ease of installation of the flux chambers, these methods have small footprint, are not suitable for long term canopy-scale CO_2 flux measurements in tall forest ecosystems and mostly used for grasslands with small canopy height or leaf, bole and soil respiration components (Law et al. 1999).

Once *NEE* is estimated by the above-mentioned methods, it is partitioned into *GPP* and *TER* using respiration (Reichstein 2005), light-use efficiency (Lasslop et al. 2010), isotopic fractionation (Bowling et al. 2001) or statistical correlation based methods (Skaggs et al. 2018).

2.2.3   Satellite Measurements

In situ measurements by far provide the most realistic estimates of the carbon cycle of terrestrial ecosystems. However, these have limited footprints. A dense network of ground-based towers instrumented with multiple sensors is required to be deployed for estimating the *NPP* of any region, as outlined in the previous section. Also the measurements need to be continued seamlessly at least for several years before a reasonable estimation can be achieved with the seasonal, intra-seasonal and inter-annual variabilities (Baldocchi 2001). Establishing such networks are challenging in remote and inaccessible locations. Moreover the ground-based measurement systems are marred by severe data loss due to power shortage, adverse weather conditions etc. Maintaining such systems required long-term dedicated effort, human involvement and have high establishment and operating costs. The data collection, processing and interpretation can be tedious for difficult terrains such as mountainous regions, dense rainforests etc. In view of these *NPP* can be remotely monitored using satellite and other remote sensing techniques as described below.

2.2.3.1   Vegetation Indices

Vegetation indices (*VI*s) are spectral transformations of the reflectances recorded by satellite sensors in multiple bands of the electromagnetic spectrum (Huete et al. 2002). These are dimensionless and used for monitoring the vegetation health and photosynthetic activities at different spatio-temporal scales. Different *VI*s are formulated such as the normalized difference vegetation index (*NDVI*), leaf area index (*LAI*), enhanced vegetation index (*EVI*), land-surface water index (*LSWI*), soil-adjusted vegetation index (*SAVI*) etc. which are used in combination with the meteorological measurements as input to the bottom-up models for predicting the *NPP* (Liu et al. 1997) or *GPP* (Deb Burman et al. 2017). The *LAI* is defined as the total one-sided leaf surface area relative to per unit ground area (Watson 1947) which can be estimated from the ground-based or satellite measurements (Bréda 2003; Deng et al. 2006). It is closely connected with *NDVI* which is estimated from the surface reflectances as defined below,

$$NDVI = \frac{\alpha_{nir} - \alpha_{vis}}{\alpha_{nir} + \alpha_{vis}} \qquad (2.15)$$

where, α_{nir} and α_{vis} are the averaged surface reflectances in the visible and near infrared regions of the electromagnetic radiation spectrum, respectively (Carlson and Ripley 1997). The *EVI* is an adaptation of *NDVI* corrected for the atmospheric and canopy background noises which is more sensitive towards dense canopies (Jiang et al. 2008). On a similar note, the *LSWI* is a modification of *NDVI* that takes care of the effect of vegetation leaf structure, moisture contents in leaf and soil on the spectral reflectances (Fensholt and Sandholt 2003; Xiao et al. 2004). The *SAVI* is a modification of *NDVI* adjusted for the soil brightness effect as defined by Huete (1988).

Different adaptations of this methodology exists in literature where the *VI* had either been estimated from the satellites such as LANDSAT (Ganguly et al. 2012), Moderate Resolution Imaging Spectroradiometer (MODIS) (Demarty et al. 2007), Advanced Very High Resolution Radiometer (AVHRR) (Buermann et al. 2001) etc. or the ground-based measurements (Deb Burman et al. 2017) and the meteorological variables are either taken from the surface measurements (Bao et al. 2016; Deb Burman et al. 2017), remote sensing observations (Sims et al. 2008), model predictions (Yan et al. 2016) or a suitable assimilation of these (Demarty et al. 2007). The functioning of bottom-up models is described in Sect. 2.2.4.1 of this chapter. The development of *VIs* from reflectances measured by the satellites is challenging due to multiple constraints, such as atmospheric scattering, vegetation structure, leaf inclination, albedo etc. (Knyazikhin et al. 1998) and hence remains to be an active area of research.

2.2.3.2   Light Use Efficiency Approach

According to Monteith (1972, 1977) the photosynthetic yield of any ecosystem is directly proportional to the amount of solar radiation absorbed by the canopy in absence of any water or nutrient stress in soil. The plants absorb solar radiation in the photosynthetically active radiation (*PAR*) or visible range of the electromagnetic spectrum (wavelength varying within 400–700 nm) (Alados et al. 1996). The amount of *PAR* absorbed by the plants is known as the absorbed photosynthetically active radiation (*APAR*) which is related to *PAR* as follows,

$$APAR = fAPAR * PAR \tag{2.16}$$

where, *fAPAR* is known as the fraction of photosynthetically active radiation. This is the basis of light use efficiency (*LUE*) approach to estimate *NPP* of any ecosystem formulated as,

$$NPP = fAPAR * PAR * \varepsilon \tag{2.17}$$

where, ε is the effective *LUE* of the ecosystem in the measured environmental condition that varies widely across the ecosystems depending on their geographical location, species type, canopy structure, presence of enzymes, evaporative demand, temperature stress, availabilities of moisture and nutrients etc. It is expressed as a downscaled fraction of the theoretical maximum *LUE*, ε_{max} as,

$$\varepsilon = \varepsilon_{max} * f \tag{2.18}$$

where the factor f accounts for the deviation of ε from ε_{max} owing to the non-optimal environmental conditions (Monteith 1972). Initially ε_{max} was largely thought be constant at $0.405 \, \text{gC MJ}^{-1}$ (Potter et al. 1993), which was later found to vary between a wider range (Ahl et al. 2004; Yu et al. 2009). Multiple models use this methodology to predict *NPP* such as the Carnegie-Ames-Stanford Approach (CASA) (Potter et al. 1993), Vegetation Photosynthesis Model (VPM) (Xiao et al. 2004), Physiological Principles for Predicting Growth (3-PG) (Coops et al. 2005) etc.

2.2.3.3   Derived Biophysical Products

Using the *LUE* approach a daily *NPP* product MOD17 is developed from the Moderate Resolution Imaging Spectroradiometer (MODIS) observations. It was shown by several researchers that compared to *NPP*, *GPP* has a better correlation with *APAR* (Raymond Hunt 1994; Prince and Goward 1995). Hence while developing the MOD17 product, the *GPP* and respiration components (including growth respiration *GR* and maintenance respiration *MR*) are calculated separately and subtracted to produce *NPP* (Running et al. 1999). The *GPP* is calculated daily directly from

the *fAPAR* measured by MODIS and *PAR* from an assimilated data product whereas the *GR* and *MR* are calculated from the carbon allometric equations of plants and *LAI* estimates by MODIS namely MOD15 (Myneni et al. 1999). The biome-specific plant-physiological parameters governing the carbon allometric equations are derived from a bottom-up model Biome-BGC (Running and Hunt 1993). The functioning of such models is discussed in 2.2.4.1 of the present chapter. The MOD17 product is validated across several in situ measurements such as FLUXNET (Running et al. 1999; Zhao et al. 2005; Turner et al. 2006).

2.2.3.4 Solar Induced Fluorescence

The Solar-Induced Fluorescence (*SIF*) stands for the part of energy released from the chlorophyll-a (expressed in the unit of W m^{-2} sr^{-1} μm^{-1}) after absorbing the *PAR*, in the light pathway of photosynthesis, apart from the electron transport and thermal energy dissipation. It has a typical wavelength range of 650–800 nm, which is larger than the absorbed radiation. The strongest peak in *SIF* spectrum occurs at around740 nm, in the far-red or near-IR regime with the second strongest peak appearing at around 685 nm, in the red zone (Meroni et al. 2009; Mohammed et al. 2019). This can be attributed to the fact that in optimum condition PSI photosystem emits preferably in near-IR whereas the PSII photosystem emits in both red and near-IR (Govindje 1995).

Globally, the *SIF* is seen to have linear dependencies with *GPP* estimates from top-down and bottom-up approaches (Zhang et al. 2014; Cui et al. 2017). In a simplistic model (Guanter et al. 2014) the *SIF* observed from space can be related to *GPP* in the following way, similar to the LUE formulation described in (2.17) as,

$$GPP = SIF(\lambda) * \frac{\varepsilon}{\varepsilon_F} \tag{2.19}$$

where, SIF(λ) corresponds to the *SIF* measurement at wavelength λ (usually taken as either of 685 or 740 nm) and ε_F is an efficiency factor for *SIF*, analogous to ε. In present times, a plethora of SIF estimates are available from different satellite-based sensors e.g. ENVironmental SATellite (ENVISAT) (Guanter et al. 2007), Greenhouse gases Observing SATellite (GOSAT) (Guanter et al. 2012), Global Ozone Monitoring Experiment-2 (GOME-2) (Joiner et al. 2013), SCanning Imaging Absorption SpectroMeter for Atmospheric CHartographY (SCIAMACHY) (Wolanin et al. 2015), Orbiting Carbon Observatory-2 (OCO-2) (Sun et al. 2017), TROPOspheric Monitoring Instrument (TROPOMI) (Köhler et al. 2018) etc. and have been used extensively in *GPP* estimation (Wagle et al. 2016; He et al. 2020). Different algorithms have been designed based the wavelength, atmospheric condition and canopy type. It is worthwhile to note that in a recent work Patel et al. (2018) found out the exponential relationship between cropland *NPP*, estimated from ground-based harvesting

estimates and 740 nm *SIF*, measured by GOME-2 over the Indo-Gangetic Plain in India which can be further exploited for *NPP* estimation and harvest yield prediction.

2.2.3.5 Other Remote Sensing Measures

In conjunction with the ground-based and satellite measurements, aircrafts (Cihlar et al. 1992; Desjardins et al. 1992; Macpherson et al. 1992; Chou et al. 2002) and unmanned aerial vehicles (Pirk et al. 2017) have been used for CO_2 flux measurements. The instrumentation of such campaigns include vertical concentration profile, EC (Oechel et al. 1998), *VI* and *SIF* (Zarco-Tejada et al. 2013) measurements. The SIF measurements have also been deployed on the ground (Grossmann et al. 2018). The working principle of these measurements remain the same as discussed earlier but additional quality control measures are implemented to account for the complexities arising in such measurements.

2.2.4 Modelling

The observations provide real time diagnostic information about the *NPP*. However for prediction of the ecosystem health and carbon sequestration in response to the changes in climate and environmental conditions prognostic information is required, which can be achieved by the models (Prentice et al. 2001; Levy et al. 2004). The models are a set of mathematical equations, algebraic, differential, integral or a combination of these to describe the coupled meteorological and ecophysiological processes. These equations are built upon the theories as well as the phenomenological relations derived from the observations (Bonan et al. 2011) and can be solved analytically or numerically. These models are tested by comparing the predicted variables against their direct observations for a certain measurement interval. This process is known as the calibration. Further a calibrated model is run again for a different time interval and the simulated output is checked against the measurement, thus validating the model (Enting and Pearman 1986; Friend et al. 2007). In a sense the models act as a bridge between the observations and predictions. There are two major modelling approaches as described below.

2.2.4.1 Bottom-Up Approach

As the name suggests, in bottom-up approach the leaf or canopy scale measurements are upscaled to local, national, regional or global scales using the biogeophysical and biogeochemical processes. Hence these models are also known as the process-based models (Ito and Oikawa 2002). The vegetation growth and decay in process-based models depend on climate forcing and environmental conditions which are improvement over the traditional land-surface models where the vegetation is prescribed

with no dynamical change (Foley et al. 1996; Clark et al. 2011; Lawrence et al. 2011). Due to this property the process-based models can be used for ecosystem growth prediction under changed climate such as crop production in a water-stressed condition (Gervois et al. 2004). Hence the process-based models are known as the dynamic global vegetation models, abbreviated as DGVM (Sitch et al. 2003; Prentice and Cowling 2013). These models can be simulated at a point or grid scale as a standalone model or a constituent module of a couple climate, general circulation or Earth system model (Zeng et al. 2002; Bonan and Levis 2006; Kato et al., 2009). Either of surface measurements, satellite products, reanalysis datasets or a suitable combination of these are used as input variables to the process-based models. The input data can be provided at multi-temporal time scales e.g. half-hourly, hourly, daily etc. (Williams et al. 1996; Deb Burman et al. 2017).

The process-based models have different components i.e. soil, ecosystem, atmosphere, hydrology etc. linked to each other by different complex feedback mechanisms which can be broadly classified into two categories namely, biogeochemistry and biogeophysics (El-Masri et al. 2013). Input variables of these models vary among different formulations. However, most of these models require meteorological parameters such as the shortwave and longwave radiations, air temperature, pressure, humidity, wind speed, precipitation, c_a etc. as input. In addition, *VI*s such as *LAI* are required by several models.

The photosynthesis in the models is parameterized according to the pathways i.e. C3 (Farquhar et al. 1980; Collatz et al. 1991), C4 (Collatz et al. 1992), CAM (Cortázar and Nobel 1990; Kluge and Ting 2012) etc. where the carbon assimilation is governed by the availability of *PAR* (Sellers et al. 1992), RuBisCO activity (Bernacchi et al. 2001), phosphophenolpyruvate (PEP)-carboxylase enzyme functionality (Vidal and Chollet 1997), electron transport capacity, leaf nitrogen content (Kattge et al. 2009) etc. In addition the air temperature, moisture demand and soil moisture also affect the carbon uptake by stomatal opening and closure resulting from heat and water stresses. The amount of *PAR* absorbed by the plants depends on leaf structure, orientation and area, incident *PAR* and albedo (Knyazikhin et al. 1998; Dai et al. 2004; Fensholt et al. 2004). The incident *PAR* can be directly measured or computed from the incoming solar radiation (Deb Burman et al. 2020a, b) whereas the leaf area is computed from *LAI*. As the carbon and water cycles are interlinked with nutrient cycles e.g. nitrogen, phosphorus etc. such models also need information regarding soil bulk density, organic matter content, texture and nutrient profiles for spin-up (Thornton and Rosenbloom 2005; Oleson et al. 2013).

A part of the total photosynthetic carbon uptake or gross primary productivity (*GPP*) is lost to the atmosphere by respiration. Different respiration components include growth and maintenance respirations of leaves, stems and roots (Barman et al. 2014a, b) which are computed from the direct temperature dependence of respiration (Ryan 1991) or a temperature dependent activation factor (Arora and Boer 2005). This approach is slightly different from the observational approach where the autotrophic and heterotrophic respirations are clubbed together as total ecosystem respiration (*TER*) and computed from the nighttime temperature dependence of F_c

by statistical regression (Lloyd and Taylor 1994). Finally the GPP is computed as the sum of *TER* and F_c.

Next, the fixed carbon is allocated among different pools i.e. root, leaf, stem, bole, litter etc. using the experimentally determined parameter values e.g. leaf area per unit carbon, leaf nitrogen content etc. (Sitch et al. 2003). A schematic of such a process-based model showing different compartments of carbon allocation and their interrelation is shown in Fig. 2.2, reprinted with permission from El-Masri et al. (2013). The plants are not modelled individually in the process-based models, as that would require much detailed parameterization and more computational resources, rather the plants are broadly categorized into several plat functional types (PFTs). Such clubbing of plants is implemented based on their photosynthesis pathway, geographical and climatological distributions such as tropical broadleaf deciduous, boreal coniferous evergreen, shrub, tundra, pasture, grassland etc. (Poulter et al.
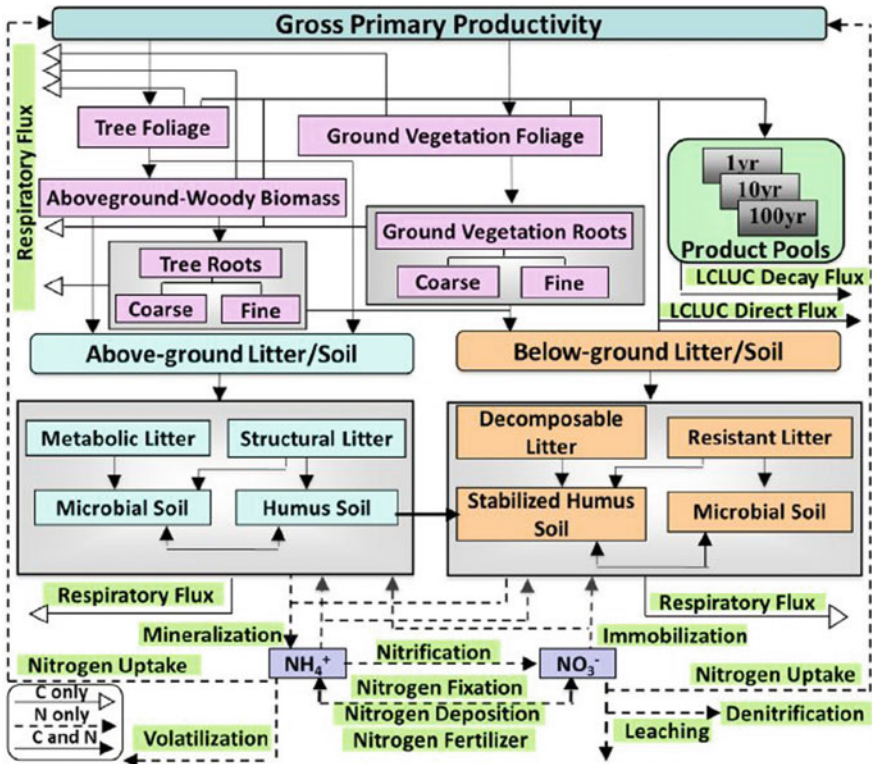
Fig. 2.2 A schematic diagram of the different carbon pools and processes in a process-based ecosystem model Integrated Science Assessment Model (ISAM) (reprinted from El-Masri et al. (2013) with permission)

2011). It is worthwhile to note here that several ecosystems remain poorly or under-represented in such models due to the lack of understanding of their ecophysiological processes owing to a lack of adequate experimental evidences or complexity in modelling those such as mangrove, rice paddy etc. (Langerwisch et al. 2018; Kumar and Scheiter 2019). For regional or global scale applications the vegetation map is prescribed to the bottom-up models as land cover and use map (Ramankutty and Foley 1999; Klein Goldewijk et al. 2011). The representativeness and accuracy of these maps remain a crucial control of uncertainty of the *NPP* estimation by these models (Arora and Boer 2010).

2.2.4.2 Top-Down Approach

The alternate approach to model the Earth-atmosphere trace gas fluxes is the top-down approach. As evident in its name, in this method the atmospheric trace gases concentrations are observed at multiple spatial and temporal scales and the sources and sinks responsible for these distributions are computed by a backward modelling approach (Gurney et al. 2004; Rayner et al. 2005). This methodology is also known as the inverse modelling which is opposite in approach to the bottom-up modelling where a forward scheme is implemented. The variables (ψ) and observations (χ) matrices are connected by the following relation,

$$G \cdot \psi = \chi \qquad (2.20)$$

where G is the coefficient matrix. The basic problem in inverse modelling lies in finding the inverse of G which is mostly calculated by Bayesian inversion (Heimann and Kaminski 1999). The observed spatio-temporal distribution of trace gases are apportioned into potential sources and sinks using atmospheric transport models (Kaminski et al. 1999) which can be solved in Lagrangian (Pisso et al. 2019), Eularian (Pillai et al. 2012) or hybrid schemes (Siqueira et al. 2000). The terrestrial sources and sinks of atmospheric CO_2 include the natural and agricultural ecosystems which are our elements of interest in the present chapter. A good knowledge of the biospheric-atmospheric CO_2 exchange, its seasonal variation and controlling parameters is required for the proper evaluation of *NEP* using inverse methods. The limited scope of the present chapter will not allow me to go into the mathematical and technical details of these techniques but the interested readers are suggested to consult the available vast scientific literature for more insight (Bousquet et al. 1999; Gurney et al. 2002; Peylin et al. 2013).

This apparently simple problem is not very straightforward in reality as I discuss next. A plethora of different sets of available data are used in inverse modelling. These include surface observations (Pickett-Heaps et al. 2011), aircraft measurements (Pisso et al. 2019), ship measurements (Bousquet et al. 1999), satellite products (Houweling et al. 2003, 2015) etc. The measurements of atmospheric traces gases concentrations and fluxes are not spread uniformly across the globe. While

some regions are well-mapped with dense observation networks with measurements carried at high temporal resolution (Bousquet et al. 1999) such as north America, some regions do not have adequate observation stations or high frequency measurements (Heimann and Kaminski 1999) such as India (Nalini et al. 2019). Aircraft measurements are costly and still limited in number like the ship observations (Patra et al. 2011). The satellite observations are often contaminated with scattering at different levels, boundary-layer dynamics and presence of clouds which are more prominent over the tropical regions (Rayner et al. 2002; Pandey et al. 2016). Together these result in the data gaps in χ.

In such cases the inverse problem becomes ill-posed with the number of observations being less than the number of control variables and an unique solution to the inverse problem ceases to exist (Heimann and Kaminski 1999). Moreover the errors in χ result in inaccurate estimation of the inverse of G. In case of Bayesian inversion the directly measured surface fluxes (Chevallier et al. 2006) or bottom-up model outputs (Dargaville et al. 2002; Patra et al. 2011) are provided to constrain the problems as a priori information of source and sink strengths. Subsequently the source and sink strength are predicted from the inverse models. These a posteriori estimates are subsequently compared with the a priori information. To reduce the uncertainty in this process a cost function is defined between the observed and simulated concentrations and a priori and a posteriori flux estimates (Kadygrov et al. 2009) which is subsequently minimized by several optimization methods used in data assimilation such as Kalman filter, 4D-var etc. (Liu et al. 2016). Apart from these the errors in transport model formulation propagate in the source and sink patterns by the inverse models (Bousquet et al. 1996; Schuh et al. 2019). The success of inverse modelling of any trace gas requires a proper understanding of the trace gas species chemistry. It has been mostly successful for long-lived trace gases such as CO_2, CH_4 etc. which take part in the long-range transport. Often to reduce the computational cost the Earth surface is divided into several regions (typically less than 100) and the average flux for each of these zones are modelled by the inverse models. A schematic of different regions used in the TRANSCOM inversion is shown in Fig. 2.3 (reprinted with permission from Houweling et al. (2015)). However such averaging reduces the spatial heterogeneity and increases the probability of misrepresentation of any region. For example it has been argued (Valsala et al. 2013) that the terrestrial biospheric CO_2 fluxes in the Carbon Tracker dataset (Peters et al. 2007) is misrepresented over the Indian subcontinent as no CO_2 measurement from this region had been used as a priori flux in the Carbon Tracker dataset due to which the flux over this region is highly biased by the emissions from neighbouring regions such as China, Korea, Kazakhstan, Indonesia etc. which belong to the same averaged spatial domains as India namely Eurasian Temperate and Asia Tropical.
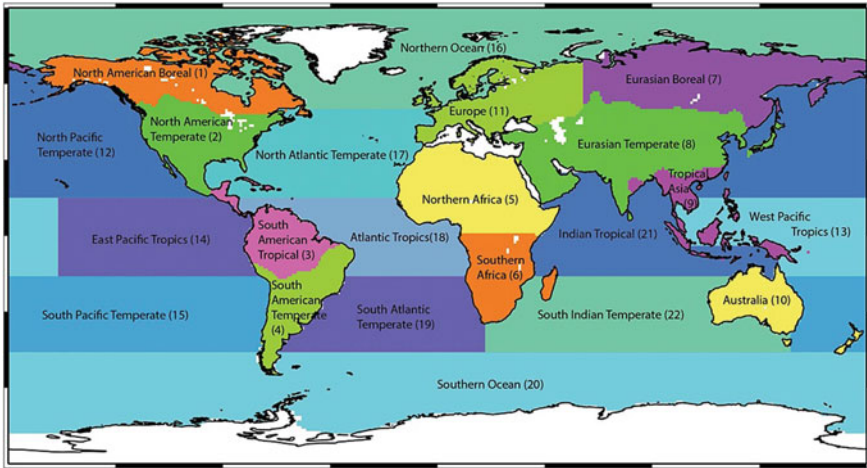
Fig. 2.3 A schematic showing the different land (and ocean) zones used in the TRANSCOM inversion (reprinted with permission from Houweling et al. (2015))

2.3 Discussion and Conclusions

Several studies have reported the different components of carbon cycle including *NPP* at global, regional and ecosystem levels using different techniques discussed above or a combination of these (Beer et al. 2010; Jung et al. 2011; Barman et al. 2014b; Tramontana et al. 2016). According to the multi-model study by Cramer et al. (1999) the global *NPP* ranges within 44.4–66.3 Gt C y^{-1}. This is shown in Fig. 2.4 which is
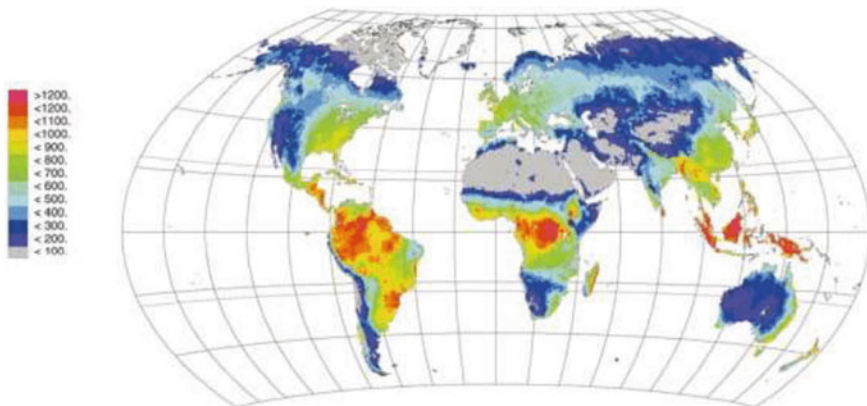
Fig. 2.4 A global map of the average annual *NPP* (gC m^{-2} y^{-1}) estimated by an ensemble of models (reprinted with permission from Cramer et al. (1999)).

reprinted from Cramer et al. (1999) with permission. Based on the MODIS measurements the average global *NPP* is 56 Gt C y^{-1}(Zhang et al. 2009). According to the combined bottom-up and top-down CO_2 data assimilation approach by Rayner et al. (2005) the global *NPP* is approximately 40.5 Gt C y^{-1}. Such studies are important to know about the sources and sinks of atmospheric CO_2 and their annual patterns. These are required not only to assess their roles in global climate change but also to predict the effect of future climate change on these ecosystems e.g. increased air temperature, increased c_a etc. However, due to the sparsity of measurements such estimates have often been riddled with lots of uncertainties both at global and regional levels (Graven et al. 2013; Patra et al. 2013; Cervarich et al. 2016). Moreover, still significant differences exist among observed, bottom-up and top-down modelled estimates of ecosystem carbon uptake (Bastos et al. 2020). In order to devise the climate change mitigation strategies the relations among plant carbon uptake and environmental variables need to be accurately known and represented in the assessment models. The terrestrial carbon cycle components predicted by the different models taking part in coupled modelintercomparison project (CMIP) (Meehl et al. 2000) differ significantly from each other due to the apparent inconsistency in the underlying land carbon cycle formulations (Anav et al. 2013; Friedlingstein et al. 2014). Such uncertainties can be reduced by improved parameterizations which can derived from the long-term measurements in the diverse ecosystem types using an optimally designed denser network of surface measurements.

References

Ahl DE, Gower ST, Mackay DS, Burrows SN, Norman JM, Diak GR (2004) Heterogeneity of light use efficiency in a northern Wisconsin forest: Implications for modeling net primary production with remote sensing. Remote Sens Environ 93(1–2):168–178. https://doi.org/10.1016/j.rse.2004.07.003

Alados I, Foyo-Moreno I, Alados-Arboledas L (1996) Photosynthetically active radiation: measurements and modelling. Agric For Meteorol 78(1–2):121–131. https://doi.org/10.1016/0168-1923(95)02245-7

Anav A, Friedlingstein P, Kidston M, Bopp L, Ciais P, Cox P, Jones C, Jung M, Myneni M, Zhu Z (2013) Evaluating the land and ocean components of the global carbon cycle in the CMIP5 earth system models. J Clim 26(1s8):6801–6843. https://doi.org/10.1175/JCLI-D-12-00417.1

Arora VK, Boer GJ (2005) A parameterization of leaf phenology for the terrestrial ecosystem component of climate models. Glob Change Biol 11:39–59. https://doi.org/10.1111/j.1365-2486.2004.00890.x

Arora VK, Boer GJ (2010) Uncertainties in the 20th century carbon budget associated with land use change. Glob Change Biol 27:3310–3348. https://doi.org/10.1111/j.1365-2486.2010.02202.x

Aubinet M, Feigenwinter C, Heinesch B, Bernhofer C, Canepa E, Lindroth A, Montagnani L, Rebmann C, Sedlak P, Van Gorsel E (2010) Direct advection measurements do not help to solve the night-time CO_2 closure problem: evidence from three different forests. Agric For Meteorol 150(5):655–664. https://doi.org/10.1016/j.agrformet.2010.01.016

Aubinet M, Vesala T, Papale D (2012) Eddy covariance: a practical guide to measurement and data analysis. Springer.

Baghi R, Durand P, Jambert C, Jarnot C, Delon C, Serça D, Keravec P (2012) A new disjunct eddy-covariance system for BVOC flux measurements—validation on CO_2 and H_2O fluxes. Atmos Meas Tech 5:3119–3132. https://doi.org/10.5194/amt-5-3119-2012

Baker JM, Norman JM, Bland WL (1992) Field-scale application of flux measurement by conditional sampling. Agric For Meteorol 62:31–52. https://doi.org/10.1016/0168-1923(92)90004-N

Baldocchi DD (2001) Assessing ecosystem carbon balance: problems and prospects of the eddy covariance technique. Ann Rev Ecol Syst

Baldocchi DD (2003) Assessing the eddy covariance technique for evaluating carbon dioxide exchange rates of ecosystems: past, present and future. Global Change Biol 9(4):479–492. https://doi.org/10.1046/j.1365-2486.2003.00629.x

Baldocchi D, Falge E, Gu L, Olson R, Hollinger D, Running S, Wofsy S (2001) FLUXNET: a new tool to study the temporal and spatial variability of ecosystem-scale carbon dioxide, water vapor, and energy flux densities. Bull Am Meteor Soc 82(February):2415–2434. https://doi.org/10.1175/1520-0477(2001)082%3c2415:FANTTS%3e2.3.CO;2

Ball JT, Woodrow IE, Berry JA (1987) A model predicting stomatal conductance and its contribution to the control of photosynthesis under different environmental conditions. In: Progress in photosynthesis research. Martinus Nijhoff Publishers, Dordrecht. https://doi.org/10.1007/978-94-017-0519-6_48

Bao G, Bao Y, Qin Z, Xin X, Bao Y, Bayarsaikan S, Chuntai B (2016) Modeling net primary productivity of terrestrial ecosystems in the semi-arid climate of the Mongolian Plateau using LSWI-based CASA ecosystem model. Int J Appl Earth Obs Geoinf 46:84–93. https://doi.org/10.1016/j.jag.2015.12.001

Barman R, Jain AK, Liang M (2014a) Climate-driven uncertainties in modeling terrestrial gross energy and water fluxes: A site level to global-scale analysis. Glob Change Biol 20(6):1885–1900

Barman R, Jain AK, Liang M (2014b) Climate-driven uncertainties in modeling terrestrial gross primary production: A site level to global-scale analysis. Glob Change Biol 20(5):1394–1411. https://doi.org/10.1111/gcb.12474

Barr AG, Richardson AD, Hollinger DY, Papale D, Arain MA, Black TA, Schaeffer K (2013) Use of change-point detection for friction-velocity threshold evaluation in eddy-covariance studies. Agric For Meteorol 171:31–45. https://doi.org/10.1016/j.agrformet.2012.11.023

Bastos A, O'Sullivan M, Ciais P, Makowski D, Sitch S, Friedlingstein P, Chevallier F, Rödenbeck C, Pongratz J, Luijkx IT, Patra PK, Peylin P, Canadell JG, Lauerwald R, Li W, Smith NE, Peters W, Goll DS, Jain AK, Kato E, Lienert S, Lombardozzi DL, Haverd V, Nabel JEMS, Poulter B, Tian H, Walker AP, Zaehle S (2020) Sources of uncertainty in regional and global terrestrial CO_2 exchange estimates. Glob Biogeochem Cycles 34(2):e2019GB006393. https://doi.org/10.1029/2019GB006393

Beer C, Reichstein M, Tomelleri E, Ciais P, Jung M, Carvalhais N, Papale D (2010) Terrestrial gross carbon dioxide uptake: Global distribution and covariation with climate. Science 329:834–838. https://doi.org/10.1126/science.1184984

Beringer J, Hutley LB, McHugh I, Arndt SK, Campbell D, Cleugh HA, Cleverly J, de Dios VS, Eamus D, Evans B, Ewenz C, Grace P, Griebel A, Haverd V, Hinko-Najera N, Huete A, Isaac P,

Kanniah K, Leuning R, Liddell MJ, Macfarlane C, Meyer W, Moore C, Pendall E, Phillips A, Phillips RL, Prober SM, Restrepo-Coupe N, Rutledge S, Schroder I, Silberstein R, Southall P, Yee MS, Tapper NJ, van Gorsel E, Vote C, Walker J, Wardlaw T (2016) An introduction to the Australian and New Zealand flux tower network—OzFlux. Biogeosciences 13(21). https://doi. org/10.5194/bg-13-5895-2016

Bernacchi CJ, Singsaas EL, Pimentel C, Portis AR, Long SP (2001) Improved temperature response functions for models of Rubisco-limited photosynthesis. Plant Cell Environ 24:2. https://doi.org/ 10.1046/j.1365-3040.2001.00668.x

Betts RA (2000) Offset of the potential carbon sink from boreal forestation by decreases in surface albedo. Nature 408:187–190. https://doi.org/10.1038/35041545

Bonan GB, Levis S (2006) Evaluating aspects of the community land and atmosphere models (CLM3 and CAM3) using a dynamic global vegetation model. J Clim 19(11):2290–2301. https:// doi.org/10.1175/JCLI3741.1

Bonan GB, Lawrence PJ, Oleson KW, Levis S, Jung M, Reichstein M, Lawrence DM, Swenson SC (2011) Improving canopy processes in the community land model version 4 (CLM4) using global flux fields empirically inferred from FLUXNET data. J Geophys Res 116. https://doi.org/ 10.1029/2010jg001593

Bongaarts J (2019) IPBES, 2019. Summary for policymakers of the global assessment report on biodiversity and ecosystem services of the Intergovernmental Science-Policy Platform on Biodiversity and Ecosystem Services. Popul Dev Rev. https://doi.org/10.1111/padr.12283

Bousquet P, Ciais P, Monfray P, Balkanski Y, Ramonet M, Tans P (1996) Influence of two atmospheric transport models on inferring sources and sinks of atmospheric CO_2. Tellus, Ser B Chem Phys Meteor 48B:568–582. https://doi.org/10.3402/tellusb.v48i4.15932

Bousquet P, Ciais P, Peylin P, Ramonet M, Monfray P (1999) Inverse modeling of annual atmospheric CO_2 sources and sinks 1. Method and control inversion. J Geophys Res Atmos 104(D21):26161–26178. https://doi.org/10.1029/1999JD900342

Bowling DR, Delany AC, Turnipseed AA, Baldocchi DD, Monson RK (1999) Modification of the relaxed eddy accumulation technique to maximize measured scalar mixing ratio differences in updrafts and downdrafts. J Geophys Res Atmos 104:9121–9133. https://doi.org/10.1029/1999JD 900013

Bowling DR, Tans PP, Monson RK (2001) Partitioning net ecosystem carbon exchange with isotopic fluxes of CO_2. Glob Change Biol 7:127–145. https://doi.org/10.1046/j.1365-2486.2001.00400.x

Bréda NJJ (2003) Ground-based measurements of leaf area index: a review of methods, instruments and current controversies. J Exp Bot 54(392):2403–2417. https://doi.org/10.1093/jxb/erg263

Buermann W, Dong J, Zeng X, Myneni RB, Dickinson RE (2001) Evaluation of the utility of satellite-based vegetation leaf area index data for climate simulations. J Clim 14:3536–3550. https://doi.org/10.1175/1520-0442(2001)014%3c3536:EOTUOS%3e2.0.CO;2

Burba G (2013) Eddy covariance method-for scientific, industrial, agricultural, and regulatory applications. Book

Burba G (2019) Illustrative maps of past and present eddy covariance measurement locations: II. High-resolution images. https://doi.org/10.13140/RG.2.2.33191.70561

Burba G, Anderson D (2007) Introduction to the eddy covariance method: general guidelines and conventional workflow. Li-Cor Biosci 141

Businger JA, Oncley SP (1990) Flux measurement with conditional sampling. J Atmos Oceanic Technol 7:349–352. https://doi.org/10.1175/1520-0426(1990)007%3c0349:fmwcs%3e2.0.co;2

Businger JA, Wyngaard JC, Izumi Y, Bradley EF (1971) Flux-profile relationships in the atmospheric surface layer. J Atmos Sci 28(2):181–189. https://doi.org/10.1175/1520-0469(1971)028%3c0 181:fprita%3e2.0.co;2

Carlson TN, Ripley DA (1997) On the relation between NDVI, fractional vegetation cover, and leaf area index. Remote Sens Environ 62(3):241–252. https://doi.org/10.1016/S0034-4257(97)001 04-1

Cervarich M, Shu S, Jain AK, Arneth A, Canadell J, Friedlingstein P, Houghton RA, Kato E, Koven C, Patra P, Poulter B, Sitch S, Stocker B, Viovy N, Wiltshire A, Zeng N (2016). The terrestrial

carbon budget of South and Southeast Asia. Environ Res Lett 11(10):105006. https://doi.org/10.1088/1748-9326/11/10/105006

Chakraborty S, Tiwari YK, Deb Burman PK, Baidya Roy S, Valsala V (2020) Observations and modeling of GHG concentrations and fluxes over India. In: Krishnan R, Sanjay J, Gnanaseelan C, Mujumdar M, Kulkarni A, Chakraborty S (eds) Assessment of climate change over the Indian region. Springer, Singapore. https://doi.org/10.1007/978-981-15-4327-2_4

Chapin FS, Woodwell GM, Randerson JT, Rastetter EB, Lovett GM, Baldocchi DD, Clark DA, Harmon ME, Schimel DS, Valentini R, Schulze ED (2006) Reconciling carbon-cycle concepts, terminology, and methods. Ecosystems. https://doi.org/10.1007/s10021-005-0105-7

Chevallier F, Viovy N, Reichstein M, Ciais P (2006) On the assignment of prior errors in Bayesian inversions of CO_2 surface fluxes. Geophys Res Lett 33(L13802). https://doi.org/10.1029/2006GL026496

Chou WW, Wofsy SC, Harriss RC, Lin JC, Gerbig C, Sachse GW (2002) Net fluxes of CO_2 in Amazonia derived from aircraft observations. J Geophys Res Atmos 107(D22):4614. https://doi.org/10.1029/2001JD001295

Cihlar J, Caramori PH, Schuepp PH, Desjardins RL, Macpherson JI (1992) Relationship between satellite-derived vegetation indices and aircraft-based CO_2 measurements. J Geophys Res 97(D17):18515–18521. https://doi.org/10.1029/92jd00655

Clark DB, Mercado LM, Sitch S, Jones CD, Gedney N, Best MJ, Pryor M, Rooney GG, Essery RLH, Blyth E, Boucher O, Harding RJ, Huntingford C, Cox PM (2011) The joint UK land environment simulator (JULES), model description—Part 2: Carbon fluxes and vegetation dynamics. Geosci Model Dev 4(3):701–722. https://doi.org/10.5194/gmd-4-701-2011

Collatz GJ, Ball JT, Grivet C, Berry JA (1991) Physiological and environmental-regulation of stomatal conductance, photosynthesis and transpiration—a model that includes a laminar boundary-layer. Agric For Meteorol 54(2–4):107–136. https://doi.org/10.1016/0168-1923(91)90002-8

Collatz GJ, Ribas-Carbo M, Berry JA (1992) Coupled photosynthesis-stomatal conductance model for leaves of C4 plants. Aust J Plant Physiol 19(1139):519–539. https://doi.org/10.1071/PP9920519

Coops NC, Waring RH, Law BE (2005) Assessing the past and future distribution and productivity of ponderosa pine in the Pacific Northwest using a process model, 3-PG. Ecol Model 183(1):107–124. https://doi.org/10.1016/j.ecolmodel.2004.08.002

Cox PM, Betts RA, Collins M, Harris PP, Huntingford C, Jones CD (2004) Amazonian forest dieback under climate-carbon cycle projections for the 21st century. Theoret Appl Climatol 78:137–156. https://doi.org/10.1007/s00704-004-0049-4

Cramer W, Kicklighter DW, Bondeau A, Iii BM, Churkina G, Nemry B, Ruimy A, Schloss AL, ThE Participants OF ThE Potsdam NpP Model Intercomparison (1999). Comparing global models of terrestrial net primary productivity (NPP): overview and key results. Glob Change Biol 5:1–15. https://doi.org/10.1046/j.1365-2486.1999.00009.x

Cui Y, Xiao X, Zhang Y, Dong J, Qin Y, Doughty RB, Zhang G, Wang J, Wu X, Qin Y, Zhou S (2017) Temporal consistency between gross primary production and solar-induced chlorophyll fluorescence in the ten most populous megacity areas over years. Sci Rep 7:14963. https://doi.org/10.1038/s41598-017-13783-5

Dai Y, Dickinson R, Wang Y (2004) A two-big-leaf model for canopy temperature, photosynthesis, and stomatal conductance. J Clim 17:2281–2299. https://doi.org/10.1175/1520-0442(2004)017%3c2281:ATMFCT%3e2.0.CO;2

Dargaville R, McGuire AD, Rayner P (2002) Estimates of large-scale fluxes in high latitudes from terrestrial biosphere models and an inversion of atmospheric CO_2 measurements. Clim Change 55:273–285. https://doi.org/10.1023/A:1020295321582

Deb Burman PK, Sarma D, Williams M, Karipot A, Chakraborty S (2017) Estimating gross primary productivity of a tropical forest ecosystem over north-east India using LAI and meteorological variables. J Earth Syst Sci 126(7):1–16. https://doi.org/10.1007/s12040-017-0874-3

Deb Burman PK, Prabha TV, Morrison R, Karipot A (2018) A case study of turbulence in the nocturnal boundary layer during the Indian summer monsoon. Bound-Layer Meteorol 169(1):115–138

Deb Burman PK, Sarma D, Morrison R, Karipot A, Chakraborty S (2019) Seasonal variation of evapotranspiration and its effect on the surface energy budget closure at a tropical forest over north-east India. J Earth Syst Sci 128(5):1–21. https://doi.org/10.1007/s12040-019-1158-x

Deb Burman PK, Sarma D, Chakraborty S, Karipot A, Jain AK (2020a) The effect of Indian summer monsoon on the seasonal variation of carbon sequestration by a forest ecosystem over North-East India. SN Appl Sci 2(2):154. https://doi.org/10.1007/s42452-019-1934-x

Deb Burman PK, Shurpali NJ, Chowdhuri S, Karipot A, Chakraborty S, Lind SE, Prabha TV (2020b) Eddy covariance measurements of CO_2 exchange from agro-ecosystems located in subtropical (India) and boreal (Finland) climatic conditions. J Earth Syst Sci 129(1):43. https://doi.org/10.1007/s12040-019-1305-4

Demarty J, Chevallier F, Friend AD, Viovy N, Piao S, Ciais P (2007) Assimilation of global MODIS leaf area index retrievals within a terrestrial biosphere model. Geophys Res Lett 34(15):L15402. https://doi.org/10.1029/2007GL030014

Deng F, Chen JM, Plummer S, Chen M, Pisek J (2006) Algorithm for global leaf area index retrieval using satellite imagery. IEEE Trans Geosci Remote Sens 44(8):2219–2229. https://doi.org/10.1109/TGRS.2006.872100

Desjardins RL (1972) A study of carbon dioxide and sensible heat fluxes using the eddy correlation technique. Cornell University

Desjardins RL, Hart RL, Macpherson JI, Schuepp PH, Verma SB (1992) Aircraft- and tower-based fluxes of carbon dioxide, latent, and sensible heat. J Geophys Res 97(D17):18477–18485. https://doi.org/10.1029/92jd01625

Dyer AJ (1974) A review of flux-profile relationships. Bound-Layer Meteorol 7(3):363–372. https://doi.org/10.1007/BF00240838

Dyer AJ, Hicks BB (1970) Flux-gradient relationships in the constant flux layer. Q J R Meteorol Soc 96(410):715–721. https://doi.org/10.1002/qj.49709641012

El-Masri B, Barman R, Meiyappan P, Song Y, Liang M, Jain AK (2013) Carbon dynamics in the Amazonian Basin : integration of eddy covariance and ecophysiological data with a land surface model. Agric For Meteorol 182–183:156–167. https://doi.org/10.1016/j.agrformet.2013.03.011

Enting IG, Pearman GI (1986) The use of observations in calibrating and validating carbon cycle models. In: The changing carbon cycle. Springer, New York. https://doi.org/10.1007/978-1-4757-1915-4_21

Etzold S, Buchmann N, Eugster W (2010) Contribution of advection to the carbon budget measured by eddy covariance at a steep mountain slope forest in Switzerland. Biogeosciences 7(8):2461–2475. https://doi.org/10.5194/bg-7-2461-2010

Falge E, Baldocchi D, Olson R, Anthoni P, Aubinet M, Bernhofer C et al (2001) Gap filling strategies for defensible annual sums of net ecosystem exchange. Agric For Meteorol 107(1):43–69. https://doi.org/10.1016/S0168-1923(00)00225-2

Farquhar GD, Sharkey TD (1982) Stomatal conductance and photosynthesis. Ann Rev Plant Physiol 33(1):317–345. https://doi.org/10.1146/annurev.pp.33.060182.001533

Farquhar GD, Von Caemmerer S, Berry JA (1980) A biochemical model of photosynthetic CO_2 assimilation in leaves of C_3 species. Planta 149:78–90. https://doi.org/10.1007/BF00386231

Fensholt R, Sandholt I (2003) Derivation of a shortwave infrared water stress index from MODIS near- and shortwave infrared data in a semiarid environment. Remote Sens Environ 87:111–121. https://doi.org/10.1016/j.rse.2003.07.002

Fensholt R, Sandholt I, Rasmussen MS (2004) Evaluation of MODIS LAI, fAPAR and the relation between fAPAR and NDVI in a semi-arid environment using in situ measurements. Remote Sens Environ 91:490–507. https://doi.org/10.1016/j.rse.2004.04.009

Foken T (2008) Micrometeorology. Micrometeorology. https://doi.org/10.1007/978-3-540-74666-9

Foken T, Göckede M, Mauder M, Mahrt L, Amiro B, Munger W (2004) Post-field data quality control. In: Handbook of micrometeorology, pp 181–208. https://doi.org/10.1007/1-4020-2265-4_9

Foley JA, Prentice IC, Ramankutty N, Levis S, Pollard D, Sitch S, Haxeltine A (1996) An integrated biosphere model of land surface processes, terrestrial carbon balance, and vegetation dynamics. Global Biogeochem Cycles 10(4):603–628. https://doi.org/10.1029/96GB02692

Friedlingstein P, Meinshausen M, Arora VK, Jones CD, Anav A, Liddicoat SK, Knutti R (2014) Uncertainties in CMIP5 climate projections due to carbon cycle feedbacks. J Clim 27(2):511–526. https://doi.org/10.1175/JCLI-D-12-00579.1

Friedlingstein P, Jones MW, Sullivan M, Andrew RM, Hauck J, Peters GP, Peters W, Pongratz J, Sitch S, Le Quéré C, Bakker DCE, Canadell JG, Ciais P, Jackson RB, Anthoni P, Barbero L, Bastos A, Bastrikov V, Becker M, Bopp L, Buitenhuis E, Chandra N, Chevallier F, Chini LP, Currie KI, Feely RA, Gehlen M, Gilfillan D, Gkritzalis T, Goll DS, Gruber N, Gutekunst S, Harris I, Haverd V, Houghton RA, Hurtt G, Ilyina T, Jain AK, Joetzjer E, Kaplan JO, Kato E, Goldewijk KK, Korsbakken JI, Landschützer P, Lauvset SK, Lefèvre N, Lenton N, Lienert S, Lombardozzi D, Marland G, McGuire PC, Melton JR, Metzl N, Munro DR, Nabel JEMS, Nakaoka S-I, Neill C, Omar AM, Ono T, Peregon A, Pierrot D, Poulter B, Rehder G, Resplandy L, Robertson E, Rödenbeck C, Séférian R, Schwinger J, Smith N, Tans PP, Tian H, Tilbrook B, Tubiello FN, van der Werf GR, Wiltshire AJ, Zaehle S (2019) Global carbon budget 2019. Earth Syst Sci Data 11(4):1783–1838. https://doi.org/10.5194/essd-11-1783-2019

Friend AD, Arneth A, Kiang NY, Lomas M, Ogee J, Rödenbeck C, Running SW, Santaren JD, Sitch S, Viovy N, Ian Woodward F (2007) FLUXNET and modelling the global carbon cycle. Global Change Biol 13(3):610–633. https://doi.org/10.1111/j.1365-2486.2006.01223.x

Gaman A, Rannik Ü, Aalto P, Pohja T, Siivola E, Kulmala M, Vesala T (2004) Relaxed eddy accumulation system for size-resolved aerosol particle flux measurements. J Atmos Oceanic Technol 21:933–943. https://doi.org/10.1175/1520-0426(2004)021%3c0933:REASFS%3e2.0.CO;2

Ganguly S, Nemani RR, Zhang G, Hashimoto H, Milesi C, Michaelis A, Wang W, Votava P, Samanta A, Melton F, Dungan JL, Vermote E, Gao F, Knyazikhin Y, Myneni RB (2012) Generating global Leaf Area Index from Landsat: algorithm formulation and demonstration. Remote Sens Environ 122:185-2-2. https://doi.org/10.1016/j.rse.2011.10.032

Garcia de Cortázar V, Nobel PS (1990) Worldwide environmental productivity indices and yield predictions for a cam plant, Opuntia ficus-indica, including effects of doubled CO_2 levels. Agric For Meteorol 49:261–279. https://doi.org/10.1016/0168-1923(90)90001-M

Geissbühler P, Siegwolf R, Eugster W (2000) Eddy covariance measurements on mountain slopes: the advantage of surface-normal sensor orientation over a vertical set-up. Bound-Layer Meteorol 96:371–392. https://doi.org/10.1023/A:1002660521017

Gervois S, de Noblet-Ducoudré N, Viovy N, Ciais P, Brisson N, Seguin B, Perrier A (2004) Including croplands in a global biosphere model: methodology and evaluation at specific sites. Earth Interact. https://doi.org/10.1175/1087-3562(2004)8%3c1:iciagb%3e2.0.co;2

Gnanamoorthy P, Selvam V, Ramasubramanian R, Nagarajan R, Chakraborty S, Deb Burman PK, Karipot A (2019) Diurnal and seasonal patterns of soil CO_2 efflux from the Pichavaram mangroves, India. Environ Monit Assess 191(4)

Gnanamoorthy P, Selvam V, Deb Burman PK, Chakraborty S, Karipot A, Nagarajan R, Ramasubramanian R, Song Q, Zhang Y, Grace J (2020) Seasonal variations of net ecosystem (CO_2) exchange in the Indian tropical mangrove forest of Pichavaram. Estuar, Coast Shelf Sci 243:106828

Govindje (1995) Sixty-three years since Kautsky: chlorophyll a fluorescence. Funct Plant Biol 22:131–160. https://doi.org/10.1071/pp9950131

Graven HD, Keeling RF, Piper SC, Patra PK, Stephens BB, Wofsy SC, Welp LR, Sweeney C, Tans PP, Kelley JJ, Daube BC, Kort EA, Santoni GW, Bent JD (2013) Enhanced seasonal exchange of CO_2 by Northern ecosystems since 1960. Science 341(6150):1085–1089. https://doi.org/10.1126/science.1239207

Grossmann K, Frankenberg C, Magney TS, Hurlock SC, Seibt U, Stutz J (2018) PhotoSpec: a new instrument to measure spatially distributed red and far-red Solar-Induced Chlorophyll Fluorescence. Remote Sens Environ 216:311–327. https://doi.org/10.1016/j.rse.2018.07.002

Guanter L, Alonso L, Gómez-Chova L, Amorós-López J, Vila J, Moreno J (2007) Estimation of solar-induced vegetation fluorescence from space measurements. Geophys Res Lett 34:L08401. https://doi.org/10.1029/2007GL029289

Guanter L, Frankenberg C, Dudhia A, Lewis PE, Gómez-Dans J, Kuze A, Suto H, Grainger RG (2012) Retrieval and global assessment of terrestrial chlorophyll fluorescence from GOSAT space measurements. Remote Sens Environ 12:236–251. https://doi.org/10.1016/j.rse.2012.02.006

Guanter L, Zhang Y, Jung M, Joiner J, Voigt M. Berry JA, Frankenberg C, Huete AR, Zarco-Tejada P, Lee J-E, Moran M-S, Ponce-Campos G, Beer C, Camps-Valls G, Buchmann N, Gianelle D, Klumpp K, Cescatti A, Bake JM, Griffis TJ (2014) Global and time-resolved monitoring of crop photosynthesis with chlorophyll fluorescence. Proc Natl Acad Sci U S A 111(14):E1327–E1333. https://doi.org/10.1073/pnas.1320008111

Guenther A, Baugh W, Davis K, Hampton G, Harley P, Klinger L, Vierling L, Zimmerman P, Allwine W, Dilts S, Lamb B, Westberg H, Baldocchi D, Geron C, Pierce T (1996) Isoprene fluxes measured by enclosure, relaxed eddy accumulation, surface layer gradient, mixed layer gradient, and mixed layer mass balance techniques. J Geophys Res Atmos 101:18555–18567. https://doi.org/10.1029/96jd00697

Gurney, K. R., Law, R. M., Denning, A. S., Rayner, P. J., Baker, D., Bousquet, P., Bruhwiler L, Chen Y-H, Ciais P, Fan S, Fung IY, Gloor M, Heimann M, Higuchi K, John K, Maki T, Maksyutov S, Masarie K, Peylin P, Prather M, Pak BC, Randerson J, Sarmiento J, Taguchi S, Takahashi T, Yuen CW (2002) Towards robust regional estimates of CO_2 sources and sinks using atmospheric transport models. Nature 415:626–629. https://doi.org/10.1038/415626a

Gurney KR, Law RM, Denning AS, Rayner PJ, Pak BC, Baker D, Bousquet P, Bruhwiler L, Chen Y-H, Ciais P, Fung IY, Heimann M, John J, Maki T, Maksyutov S, Peylin P, Prather M, Taguchi, S. (2004). Transcom 3 inversion intercomparison: Model mean results for the estimation of seasonal carbon sources and sinks. Global Biogeochem Cycles 18(1):GB1010. https://doi.org/10.1029/2003gb002111

Gu L, Falge EM, Boden T, Baldocchi DD, Black TA, Saleska SR, Suni T, Verma SB, Vesala T, Wofsy SC, Xu L (2005) Objective threshold determination for nighttime eddy flux filtering. Agric For Meteorol 128(3–4):179–197. https://doi.org/10.1016/j.agrformet.2004.11.006

Heimann M, Kaminski T (1999) Inverse modelling approaches to infer surface trace gas fluxes from observed atmospheric mixing ratios. In Approaches to scaling a trace gas fluxes in ecosystems. Elsevier B.V., p. 2770295. https://doi.org/10.1016/S0167-5117(98)80035-9

He L, Magney T, Dutta D, Yin Y, Köhler P, Grossmann K, Stutz J, Dold C, Hatfield J, Guan K, Peng B, Frankenberg C (2020) From the ground to space: using solar-induced chlorophyll fluorescence to estimate crop productivity. Geophys Res Lett 47(7):e2020GL087474. https://doi.org/10.1029/2020GL087474

Hicks BB, McMillen RT (1984) A simulation of the Eddy accumulation method for measuring pollutant fluxes. J Climate Appl Meteorol 23:637–643. https://doi.org/10.1175/1520-0450(1984)023%3c0637:ASOTEA%3e2.0.CO;2

Hörtnagl L, Clement R, Graus M, Hammerle A, Hansel A, Wohlfahrt G (2010) Dealing with disjunct concentration measurements in eddy covariance applications: a comparison of available approaches. Atmos Environ 44:2024–2032. https://doi.org/10.1016/j.atmosenv.2010.02.042

Houweling S, Breon F-M, Aben I, Rödenbeck C, Gloor M, Heimann M, Ciais P (2003) Inverse modeling of CO_2 sources and sinks using satellite data: a synthetic inter-comparison of measurement techniques and their performance as a function of space and time. Atmos Chem Phys Discuss 4:523–538. https://doi.org/10.5194/acpd-3-5237-2003

Houweling S, Baker D, Basu S, Boesch H, Butz A, Chevallier F, Deng F, Dlugokencky EJ, Feng L, Ganshin A, Hasekamp O (2015). An intercomparison of inverse models for estimating sources and sinks of CO_2 using GOSAT measurements. J Geophys Res 120:5253–5266. https://doi.org/10.1002/2014JD022962

Huete AR (1988) A soil-adjusted vegetation index (SAVI). Remote Sens Environ 25:295–309. https://doi.org/10.1016/0034-4257(88)90106-X

Huete A, Didan K, Miura T, Rodriguez EP, Gao X, Ferreira LG (2002) Overview of the radiometric and biophysical performance of the MODIS vegetation indices. Remote Sens Environ 83:195–213. https://doi.org/10.1016/S0034-4257(02)00096-2

IPCC (2013) Climate Change 2013: The Physical Science Basis. Contribution of Working Group I to the Fifth Assessment Report of the Intergovernmental Panel on Climate Change [Stocker TF, Qin D, Plattner G-K, Tignor M, Allen SK, Boschung J, Nauels A, Xia Y, Bex V, Midgley PM (eds)]. Cambridge University Press, Cambridge, United Kingdom and New York, NY, USA, 1535 pp

IPCC (2019) Climate Change and Land: an IPCC special report on climate change, desertification, land degradation, sustainable land management, food security, and greenhouse gas fluxes in terrestrial ecosystems [Shukla PR, Skea J, Calvo Buendia E, Masson-Delmotte V, Pörtner H-O, Roberts DC, Zhai P, Slade R, Connors S, van Diemen R, Ferrat M, Haughey E, Luz S, Neogi S, Pathak M, Petzold J, Portugal Pereira J, Vyas P, Huntley E, Kissick K, Belkacemi M, Malley J (eds)]. In press

Ito A, Oikawa T (2002) A simulation model of the carbon cycle in land ecosystems (Sim-CYCLE): A description based on dry-matter production theory and plot-scale validation. Ecol Model 151:143–176. https://doi.org/10.1016/S0304-3800(01)00473-2

Jarvis PG (1976) The interpretation of the variations in leaf water potential and stomatal conductance found in canopies in the field. Philos Trans R Soc Lond B, Biol Sci 273(927):593–610. https://doi.org/10.1098/rstb.1976.0035

Jiang Z, Huete AR, Didan K, Miura T (2008) Development of a two-band enhanced vegetation index without a blue band. Remote Sens Environ 112(10):3833–3845. https://doi.org/10.1016/j.rse.2008.06.006

Joiner J, Guanter L, Lindstrot R, Voigt M, Vasilkov AP, Middleton EM, Huemmrich KF, Yoshida Y, Frankenberg C (2013) Global monitoring of terrestrial chlorophyll fluorescence from moderate-spectral-resolution near-infrared satellite measurements: methodology, simulations, and application to GOME-2. Atmos Meas Tech 6:2803–2823. https://doi.org/10.5194/amt-6-2803-2013

Jung M, Reichstein M, Margolis HA, Cescatti A, Richardson AD, Arain MA, Arneth A, Bernhofer C, Bonal D, Chen J, Gianelle D, Gobron N, Kiely G, Kutsch W, Lasslop G, Law BE, Lindroth A, Merbold L, Montagnani L, Moors EJ, Papale D, Sottocornola M, Vaccari F, Williams C (2011) Global patterns of land-atmosphere fluxes of carbon dioxide, latent heat, and sensible heat derived from eddy covariance, satellite, and meteorological observations. J Geophys Res Biogeosci 116(3):2–4. https://doi.org/10.1029/2010JG001566

Kadygrov N, Maksyutov S, Eguchi N, Aoki T, Nakazawa T, Yokota T, Inoue G (2009) Role of simulated GOSAT total column CO_2 observations in surface CO_2 flux uncertainty reduction. J Geophys Res: Atmos 114(D21)

Kaimal JC, Finnigan JJ (1994) Atmospheric boundary layer flows: their structure and measurement. Oxford University Press

Kaminski T, Heimann M, Giering R (1999) A coarse grid three-dimensional global inverse model of the atmospheric transport 1. Adjoint model and Jacobian matrix. J Geophys Res Atmos 104(D15):18535–18553. https://doi.org/10.1029/1999JD900147

Kato T, Ito A, Kawamiya M (2009) Multiple temporal scale variability during the twentieth century in global carbon dynamics simulated by a coupled climate—terrestrial carbon cycle model. Clim Dyn 32:901–923. https://doi.org/10.1007/s00382-009-0548-1

Kattge J, Knorr W, Raddatz T, Wirth C (2009) Quantifying photosynthetic capacity and its relationship to leaf nitrogen content for global-scale terrestrial biosphere models. Glob Change Biol 15:976–991. https://doi.org/10.1111/j.1365-2486.2008.01744.x

Klein Goldewijk K, Beusen A, Van Drecht G, De Vos M (2011) The HYDE 3.1 spatially explicit database of human-induced global land-use change over the past 12,000 years. Global Ecol Biogeograp 20(1):73–86. https://doi.org/10.1111/j.1466-8238.2010.00587.x

Kljun N, Calanca P, Rotach MW, Schmid HP (2015) A simple two-dimensional parameterisation for Flux Footprint Prediction (FFP). Geosci Model Dev 8(11):3695–3713. https://doi.org/10.5194/gmd-8-3695-2015

Kluge M, Ting IP (2012) Crassulacean acid metabolism: analysis of an ecological adaptation, 30th edn. Springer, Berlin. https://doi.org/10.1007/978-3-642-67038-1

Knyazikhin Y, Martonchik JV, Myneni RB, Diner DJ, Running SW (1998) Synergistic algorithm for estimating vegetation canopy leaf area index and fraction of absorbed photosynthetically active radiation from MODIS and MISR data. J Geophys Res Atmos 103:32257–32275. https://doi.org/10.1029/98JD02462

Köhler P, Frankenberg C, Magney TS, Guanter L, Joiner J, Landgraf J (2018) Global retrievals of solar-induced chlorophyll fluorescence with TROPOMI: first results and intersensor comparison to OCO-2. Geophys Res Lett 45(19):10456–10463. https://doi.org/10.1029/2018GL079031

Kormann R, Meixner FX (2001) An analytical footprint model for non-neutral stratification. Bound-Layer Meteorol 99(2):207–224. https://doi.org/10.1023/A:1018991015119

Kumar D, Scheiter S (2019) Biome diversity in South Asia—how can we improve vegetation models to understand global change impact at regional level? Sci Total Environ 671:1001–1016. https://doi.org/10.1016/j.scitotenv.2019.03.251

Kutsch WL, Bahn M, Heinemeyer A (2010) Soil carbon dynamics: an integrated methodology. https://doi.org/10.1017/CBO9780511711794

Langerwisch F, Vaclavik T, Von Bloh W, Vetter T, Thonicke K (2018) Combined effects of climate and land-use change on the provision of ecosystem services in rice agro-ecosystems. Environ Res Lett 13:015003. https://doi.org/10.1088/1748-9326/aa954d

Lasslop G, Reichstein M, Papale D, Richardson AD, Arneth A, Barr A, Stoy P, Wohlfahrt G (2010) Separation of net ecosystem exchange into assimilation and respiration using a light response curve approach : critical issues and global evaluation. Global Change Biol 16(1):187–208. https://doi.org/10.1111/j.1365-2486.2009.02041.x

Law BE, Ryan MG, Anthoni PM (1999) Seasonal and annual respiration of a ponderosa pine ecosystem. Glob Change Biol 5(2):169–182

Lawrence DM, Oleson KW, Flanner MG, Thornton PE, Swenson SC, Lawrence PJ, Slater AG (2011) Parameterization improvements and functional and structural advances in Version 4 of the Community Land Model. J Adv Model Earth Syst 3(1). https://doi.org/10.1029/2011ms000045

Lee X (2018) Fundamentals of boundary-layer meteorology. Springer, Cham, Switzerland. https://doi.org/10.1007/978-3-319-60853-2

Leuning R (1990) Modelling stomatal behaviour and and photosynthesis of *Eucalyptus grandis*. Funct Plant Biol 17(2):159–175. https://doi.org/10.1071/pp9900159

Levy PE, Cannell MGR, Friend AD (2004) Modelling the impact of future changes in climate, CO_2 concentration and land use on natural ecosystems and the terrestrial carbon sink. Global Environ Change 14:21–30. https://doi.org/10.1016/j.gloenvcha.2003.10.005

Liu J, Chen JM, Cihlar J, Park WM (1997) A process-based boreal ecosystem productivity simulator using remote sensing inputs. Remote Sens Environ 62:158–175. https://doi.org/10.1016/S0034-4257(97)00089-8

Liu J, Bowman KW, Lee M (2016) Comparison between the local ensemble transform kalman filter (LETKF) and 4D-Var in atmospheric CO_2 flux inversion with the goddard earth observing system-chem model and the observation impact diagnostics from the LETKF. J Geophys Res 121:13066–13087. https://doi.org/10.1002/2016JD025100

Lloyd J, Taylor JA (1994) On the temperature dependence of soil respiration. Funct Ecol 8(3):315. https://doi.org/10.2307/2389824

Macpherson JI, Grossman RL, Kelly RD (1992) Intercomparison results for FIFE flux aircraft. J Geophys Res 97(D17):18499–18514. https://doi.org/10.1029/92jd00272

Massman WJ, Lee X (2002) Eddy covariance flux corrections and uncertainties in long-term studies of carbon and energy exchanges. Agric For Meteorol 113(1–4):121–144. https://doi.org/10.1016/S0168-1923(02)00105-3

Mauder M, Cuntz M, Drüe C, Graf A, Rebmann C, Schmid HP, Schmidt M, Steinbrecher R (2013) A strategy for quality and uncertainty assessment of long-term eddy-covariance measurements. Agric For Meteorol 169:122–135. https://doi.org/10.1016/j.agrformet.2012.09.006

Meehl GA, Boer GJ, Covey C, Latif M, Stouffer RJ (2000) The coupled model intercomparison project (CMIP). Bull Am Meteor Soc 81(2):313–318. https://doi.org/10.1175/1520-0477(2000)081%3c0313:tcmipc%3e2.3.co;2

Meroni M, Rossini M, Guanter L, Alonso L, Rascher U, Colombo R, Moreno J (2009) Remote sensing of solar-induced chlorophyll fluorescence: review of methods and applications. Remote Sens Environ 113:2037–2051. https://doi.org/10.1016/j.rse.2009.05.003

Meyers TP, Hall ME, Lindberg SE, Kim K (1996) Use of the modified Bowen-ratio technique to measure fluxes of trace gases. Atmos Environ 30(19):3321–3329. https://doi.org/10.1016/1352-2310(96)00082-9

Milne R, Beverland IJ, Hargreaves K, Moncrieff JB (1999) Variation of the β coefficient in the relaxed eddy accumulation method. Bound-Layer Meteorol 93:221–225. https://doi.org/10.1023/A:1002061514948

Minx JC, Lamb WF, Callaghan MW, Fuss S, Hilaire J, Creutzig F, Amann T, Beringer T, de Oliveira Garcia W, Hartmann J, Khanna T, Lenzi D, Luderer G, Nemet GF, Rogelj J, Smith P, Vicente JLV, Wilcox J, Del Mar Zamora Dominguez M (2018) Negative emissions—Part 1: Research landscape and synthesis. Environ Res Lett 13:063001. https://doi.org/10.1088/1748-9326/aabf9b

Moffat AM, Papale D, Reichstein M, Hollinger DY, Richardson AD, Barr AG, Beckstein C, Braswell BH, Churkina G, Desai AR, Falge E (2007) Comprehensive comparison of gap-filling techniques for eddy covariance net carbon fluxes. Agric For Meteorol 147(3):209–232. https://doi.org/10.1016/j.agrformet.2007.08.011

Mohammed GH, Colombo R, Middleton EM, Rascher U, van der Tol C, Nedbal L, Goulas Y, Pérez-Priego O, Damm A, Meroni M, Joiner J, Cogliati S, Verhoef W, Malenovský Z, Gastellu-Etchegorry J-P, Miller JR, Guanter L, Moreno J, Moya I, Berry JA, Frankenberg C, Zarco-Tejada PJ (2019) Remote sensing of solar-induced chlorophyll fluorescence (SIF) in vegetation: 50 years of progress. Remote Sens Environ. https://doi.org/10.1016/j.rse.2019.04.030

Moncrieff JB, Massheder JM, De Bruin H, Elbers J, Friborg T, Heusinkveld B, Kabat P, Scott S, Søgaard H, Verhoef A (1997) A system to measure surface fluxes of momentum, sensible heat, water vapour and carbon dioxide. J Hydrol 188:589–611.

Moncrieff J, Clement R, Finnigan J, Meyers T (2004) Averaging, detrending, and filtering of eddy covariance time series. In: Handbook of micrometeorology, pp 7–31. https://doi.org/10.1007/1-4020-2265-4_2

Monteith JL et al (1965) Evaporation and environment. In: Symposia of the society for experimental biology, vol 19, p 4

Monteith JL (1972) Solar radiation and productivity in tropical ecosystems. J Appl Ecol 9(3):747–766. https://doi.org/10.2307/2401901

Monteith JL (1977) Climate and the efficiency of crop production in Britain. *Philosophical Transactions of the Royal Society of London. B, Biological Sciences*, *281*(980), 277–294. https://doi.org/10.1098/rstb.1977.0140

Myles L, Meyers TP, Robinson L (2007) Relaxed eddy accumulation measurements of ammonia, nitric acid, sulfur dioxide and particulate sulfate dry deposition near Tampa, FL, USA. Environ Res Lett 2(3):034004. https://doi.org/10.1088/1748-9326/2/3/034004

Myneni RB, Knyazikhin Y, Privette JL, Running SW, Nemani R, Zhang Y, et al (1999) MODIS Leaf Area Index (LAI) and Fraction of Photosynthetically Active Radiation absorbed by vegetation (FPAR) product. Algorithm Theoretical Basis Document. https://eospso.gsfc.nasa.gov/atbd/modistables.html

Nalini K, Sijikumar S, Valsala V, Tiwari YK, Ramachandran R (2019) Designing surface CO2 monitoring network to constrain the Indian land fluxes. Atmos Environ 218:117003. https://doi.org/10.1016/j.atmosenv.2019.117003

Oechel WC, Vourlitis GL, Brooks S, Crawford TL, Dumas E (1998) Intercomparison among chamber, tower, and aircraft net CO_2 and energy fluxes measured during the Arctic System Science

Land-Atmosphere-Ice Interactions (ARCSS-LAII) Flux Study. J Geophys Res 103(D22):28993–29903. https://doi.org/10.1029/1998JD200015

Ohkubo S, Kosugi Y, Takanashi S, Mitani T, Tani M (2007) Comparison of the eddy covariance and automated closed chamber methods for evaluating nocturnal CO_2 exchange in a Japanese cypress forest. Agric For Meteorol 142:50–65. https://doi.org/10.1016/j.agrformet.2006.11.004

Oleson KW, Lawrence DM, Bonan GB, Drewniak B (2013) Technical description of version 4.5 of the Community Land Model (CLM). https://doi.org/10.5065/D6RR1W7M

Pandey S, Houweling S, Krol M, Aben I, Chevallier F, Dlugokencky EJ, Gatti LV, Gloor E, Miller JB, Detmers R, Machida T, Röckmann T (2016) Inverse modeling of GOSAT-retrieved ratios of total column CH_4 and CO_2 for 2009 and 2010. Atmos Chem Phys 16:5043–5062. https://doi.org/10.5194/acp-16-5043-2016

Patel NR, Padalia H, Devadas R, Huete A, Senthil Kumar A, Krishna Murthy YVN (2018) Estimating net primary productivity of croplands in Indo-Gangetic Plains using GOME-2 sun-induced fluorescence and MODIS NDVI. Curr Sci 114(6):1333–1337. https://doi.org/10.18520/cs/v114/i06/1333-1337

Patra PK, Niwa Y, Schuck TJ, Brenninkmeijer CAM, MacHida T, Matsueda H, Sawa Y (2011) Carbon balance of South Asia constrained by passenger aircraft CO_2 measurements. Atmos Chem Phys 11(9):4163–4175. https://doi.org/10.5194/acp-11-4163-2011

Patra PK, Canadell JG, Houghton RA, Piao SL, Oh NH, Ciais P, Manjunath KR, Chhabra A, Wang T, Bhattacharya T, Bousquet P, Hartman J, Ito A, Mayorga E, Niwa Y, Raymond PA, Sarma VVSS, Lasco R (2013) The carbon budget of South Asia. Biogeosciences 10(1):513–527. https://doi.org/10.5194/bg-10-513-2013

Pattey E, Desjardins RL, Rochette P (1993) Accuracy of the relaxed eddy-accumulation technique, evaluated using CO_2 flux measurements. Bound-Layer Meteorol 66:341–355. https://doi.org/10.1007/BF00712728

Paw UKT, Baldocchi DD, Meyers TP, Wilson KB (2000) Correction of eddy-covariance measurements incorporating both advective effects and density fluxes. Bound-Layer Meteorol 97:487–511. https://doi.org/10.1023/A:1002786702909

Peters W, Jacobson AR, Sweeney C, Andrews AE, Conway TJ, Masarie K, Miller JB, Bruhwiler LMP, Petron G, Hirsch AI, Worthy DEJ, van der Werf GR, Randerson JT, Wennberg PO, Krol MC, Tans PP (2007) An atmospheric perspective on North American carbon dioxide exchange: CarbonTracker. Proc Natl Acad Sci U S A 104(48):18925–18930. https://doi.org/10.1073/pnas.0708986104

Peylin P, Law RM, Gurney KR, Chevallier F, Jacobson AR, Maki T, Niwa Y, Patra PK, Peters W, Rayner PJ, Rödenbeck C, van der Laan-Luijkx IT, Zhang X (2013) Global atmospheric carbon budget: results from an ensemble of atmospheric CO_2 inversions. Biogeosciences 10:6699–6720. https://doi.org/10.5194/bg-10-6699-2013

Pickett-Heaps CA, Rayner PJ, Law RM, Ciais P, Patra PK, Bousquet P, Peylin P, Maksyutov S, Marshall J, Rödenbeck C, Langenfelds RL, Steele LP, Francey RJ, Tans P, Sweeney C (2011) Atmospheric CO_2 inversion validation using vertical profile measurements: analysis of four independent inversion models. J Geophys Res Atmos 116(D12305):1–17. https://doi.org/10.1029/2010JD014887

Pillai D, Gerbig C, Kretschmer R, Beck V, Karstens U, Neininger B, Heimann M (2012) Comparing Lagrangian and Eulerian models for CO_2 transport-a step towards Bayesian inverse modeling using WRF/STILT-VPRM. Atmos Chem Phys 12:8979–8991. https://doi.org/10.5194/acp-12-8979-2012

Pirk N, Sievers J, Mertes J, Parmentier FJW, Mastepanov M, Christensen TR (2017) Spatial variability of CO_2 uptake in polygonal tundra: Assessing low-frequency disturbances in eddy covariance flux estimates. Biogeosciences 14(12):3157–3169. https://doi.org/10.5194/bg-14-3157-2017

Pisso I, Patra P, Takigawa M, Machida T, Matsueda H, Sawa Y (2019) Assessing Lagrangian inverse modelling of urban anthropogenic CO_2 fluxes using in situ aircraft and ground-based

measurements in the Tokyo area. Carbon Balance Manage 14(6):1–23. https://doi.org/10.1186/s13021-019-0118-8

Potter CS, Randerson JT, Field CB, Matson PA, Vitousek PM, Mooney HA, Klooster SA (1993) Terrestrial ecosystem production: a process model based on global satellite and surface data. Global Biogeochem Cycles 7(4):811–841. https://doi.org/10.1029/93GB02725

Poulter B, Ciais P, Hodson E, Lischke H, Maignan F, Plummer S, Zimmermann NE (2011) Plant functional type mapping for earth system models. Geosci Model Dev 4:993–1010. https://doi.org/10.5194/gmd-4-993-2011

Prentice IC, Cowling SA (2013). Dynamic global vegetation models. In: Encyclopedia of biodiversity: Second Edition. https://doi.org/10.1016/B978-0-12-384719-5.00412-3

Prentice I, Farquhar G, Fasham, M. (2001). The carbon cycle and atmospheric carbon dioxide. In: Climate change 2001: the scientific basis. https://doi.org/10.1256/004316502320517344

Prince SD, Goward SN (1995) Global primary production: a remote sensing approach. J Biogeogr 22(4):815–835

Ramankutty N, Foley JA (1999) Estimating historical changes in global land cover: croplands from 1700 to 1992. Global Biogeochem Cycles 13(4):997–1027. https://doi.org/10.1029/1999GB900046

Raymond Hunt E (1994) Relationship between woody biomass and PAR conversion efficiency for estimating net primary production from NDVI. Int J Remote Sens 15(8):1725–1729. https://doi.org/10.1080/01431169408954203

Rayner PJ, Law RM, O'Brien DM, Butler TM, Dilley AC (2002) Global observations of the carbon budget 3. Initial assessment of the impact of satellite orbit, scan geometry, and cloud on measuring CO_2 from space. J Geophys Res Atmos 107(D21):4557. https://doi.org/10.1029/2001JD000618

Rayner PJ, Scholze M, Knorr W, Kaminski T, Giering R, Widmann H (2005) Two decades of terrestrial carbon fluxes from a carbon cycle data assimilation system (CCDAS). Global Biogeochem Cycles 19:GB2026. https://doi.org/10.1029/2004GB002254

Rebmann C, Aubinet M, Schmid H, Arriga N, Aurela M, Burba, G., Clement R, De Ligne A, Fratini G, Gielen B, Grace J, Graf A, Gross P, Haapanala S, Herbst M, Hörtnagl L, Ibrom A, Joly L, Kljun N, Kolle O, Kowalski A, Lindroth A, Loustau D, Mammarella I, Mauder M, Merbold L, Metzger S, Mölder M, Montagnani L, Papale D, Pavelka M, Peichl M, Roland M, Serrano-Ortiz P, Siebicke L, Steinbrecher R, Tuovinen J-P, Vesala T, Wohlfahrt G, Franz D (2018) ICOS eddy covariance flux-station site setup: a review. Int Agrophys 32(4):471–494. https://doi.org/10.1515/intag-2017-0044

Reichstein M (2005) On the separation of net ecosystem exchange into assimilation and ecosystem respiration: review and improved algorithm. Glob Change Biol 11:1–16

Reynolds O (1895) IV. On the dynamical theory of incompressible viscous fluids and the determination of the criterion. Philos Trans R Soc Lond A 186:123–164. https://doi.org/10.1098/rsta.1895.0004

Rinne HJI, Guenther AB, Warneke C, De Gouw JA, Luxembourg SL (2001) Disjunct eddy covariance technique for trace gas flux measurements. Geophys Res Lett 28:3139–3142. https://doi.org/10.1029/2001GL012900

Running SW, Hunt ER (1993) Generalization of a Forest Ecosystem Process Model for Other Biomes, BIOME-BGC, and an Application for Global-Scale Models. Scal Physiol Process. https://doi.org/10.1016/b978-0-12-233440-5.50014-2

Running SW, Investigator P, Nemani R, Investigator A, Glassy JM, Engineer S, Thornton PE (1999) Modis daily photosynthesis (PSN) and annual net primary production (NPP) product. Algorithm theoretical basis Document

Ryan MG (1991) Effects of climate change on plant respiration. Ecol Appl 1(2):157–167. https://doi.org/10.2307/1941808

Schuh AE, Jacobson AR, Basu S, Weir B, Baker D, Bowman K, Chevallier F, Crowell S, Davis KJ, Deng F, Denning S, Feng L, Jones D, Liu J, Palmer PI (2019) Quantifying the impact of atmospheric transport uncertainty on CO_2 surface flux estimates. Global Biogeochem Cycles 33:484–500. https://doi.org/10.1029/2018GB006086

Sellers PJ, Berry JA, Collatz GJ, Field CB, Hall FG (1992) Canopy reflectance, photosynthesis, and transpiration. III. A reanalysis using improved leaf models and a new canopy integration scheme. Remote Sens Environ 42(3):187–216. https://doi.org/10.1016/0034-4257(92)90102-P

Sims DA, Rahman AF, Cordova VD, El-Masri BZ, Baldocchi DD, Bolstad PV, Flanagan L, Goldstein A, Hollinger D, Xu L (2008) A new model of gross primary productivity for North American ecosystems based solely on the enhanced vegetation index and land surface temperature from MODIS. Remote Sens Environ 112:1633–1646. https://doi.org/10.1016/j.rse.2007.08.004

Siqueira M, Lai CT, Katul G (2000) Estimating scalar sources, sinks, and fluxes in a forest canopy using Lagrangian, Eulerian, and hybrid inverse models. J Geophys Res Atmos 105(D24):29475–29488. https://doi.org/10.1029/2000JD900543

Sitch S, Smith B, Prentice IC, Arneth A, Bondeau A, Cramer W, Kaplan JO, Levis S, Lucht W, Sykes MT, Thonicke K, Venevsky S (2003) Evaluation of ecosystem dynamics, plant geography and terrestrial carbon cycling in the LPJ dynamic global vegetation model. Global Change Biol 9:161–185. https://doi.org/10.1046/j.1365-2486.2003.00569.x

Skaggs TH, Anderson RG, Alfieri JG, Scanlon TM, Kustas WP (2018) Fluxpart: open source software for partitioning carbon dioxide and water vapor fluxes. Agric For Meteorol 253–254:218–224. https://doi.org/10.1016/j.agrformet.2018.02.019

Stewart JB (1988) Modelling surface conductance of pine forest. Agric For Meteorol 43(1):19–35. https://doi.org/10.1016/0168-1923(88)90003-2

Stull RB (1988) An introduction to boundary layer meteorology, vol 13. Springer, Dordrecht. https://doi.org/10.1007/978-94-009-3027-8

Sun Y, Frankenberg C, Wood JD, Schimel DS, Jung M, Guanter L, Drewry DT, Verma M, Porcar-Castell A, Griffis TJ, Gu L, Magney TS, Köhler P, Evans B, Yuen K (2017) OCO-2 advances photosynthesis observation from space via solar-induced chlorophyll fluorescence. Science 358(6360):eaam5747. https://doi.org/10.1126/science.aam5747

Thornton PE, Rosenbloom NA (2005) Ecosystem model spin-up: Estimating steady state conditions in a coupled terrestrial carbon and nitrogen cycle model. Ecol Model 189:25–48. https://doi.org/10.1016/j.ecolmodel.2005.04.008

Tramontana G, Jung M, Schwalm CR, Ichii K, Camps-Valls G, Ráduly B., Reichstein M, Altaf Arain M, Cescatti A, Kiely G, Merbold L, Serrano-Ortiz P, Sickert S, Wolf S, Papale D (2016) Predicting carbon dioxide and energy fluxes across global FLUXNET sites with regression algorithms. Biogeosciences 13:4291–4313. https://doi.org/10.5194/bg-13-4291-2016

Turner DP, Ritts WD, Cohen WB, Gower ST, Running SW, Zhao M, Costa MH, Kirschbaum AA, Ham JM, Saleska SR, Ahl DE (2006) Evaluation of MODIS NPP and GPP products across multiple biomes. Remote Sens Environ 102:282–292. https://doi.org/10.1016/j.rse.2006.02.017

Tuzet A, Perrier A, Leuning R (2003) A coupled model of stomatal conductance, photosynthesis and transpiration. Plant, Cell Environ 26:1097–1116. https://doi.org/10.1046/j.1365-3040.2003.01035.x

Valentini R, Greco S, Seufert G, Bertin N, Ciccioli P, Cecinato A, Brancaleoni E, Frattoni M (1997) Fluxes of biogenic VOC from Mediterranean vegetation by trap enrichment relaxed eddy accumulation. Atmos Environ 31:229–238. https://doi.org/10.1016/S1352-2310(97)00085-X

Valsala V, Tiwari YK, Pillai P, Roxy M, Maksyutov S, Murtugudde R (2013) Intraseasonal variability of terrestrial biospheric CO_2 fluxes over India during summer monsoons. J Geophys Res Biogeosci 118(2):752–769. https://doi.org/10.1002/jgrg.20037

Vickers D, Mahrt L (1997) Quality control and flux sampling problems for tower and aircraft data. J Atmos Oceanic Technol 14:512–526. https://doi.org/10.1175/1520-0426(1997)014%3c0512:QCAFSP%3e2.0.CO;2

Vidal J, Chollet R (1997) Regulatory phosphorylation of C4 PEP carboxylase. Trends Plant Sci 2(6):230–237. https://doi.org/10.1016/S1360-1385(97)89548-9

Wagle P, Zhang Y, Jin C, Xiao X (2016) Comparison of solar-induced chlorophyll fluorescence, light-use efficiency, and process-based GPP models in maize. Ecol Appl 26(4):1211–1222. https://doi.org/10.1890/15-1434

Wang M, Guan DX, Han SJ, Wu JL (2010) Comparison of eddy covariance and chamber-based methods for measuring CO2 flux in a temperate mixed forest. Tree Physiol 30:149–163. https://doi.org/10.1093/treephys/tpp098

Watson DJ (1947) Comparative physiological studies on the growth of field crops: I. Variation in net assimilation rate and leaf area between species and varieties, and within and between years. Ann Botany 11(41):41–76. https://doi.org/10.1093/oxfordjournals.aob.a083148

Whitley R, Zeppel M, Armstrong N, Macinnis-Ng C, Yunusa I, Eamus D (2008) A modified Jarvis-Stewart model for predicting stand-scale transpiration of an Australian native forest. Plant Soil 305:35–47. https://doi.org/10.1007/s11104-007-9399-x

Williams M, Rastetter EB, Fernandes DN, Goulden ML (1996) Modelling the soil-plant-atmosphere continuum in a Quercus-Acer stand at Harvard Forest: the regulation of stomatal conductance by light, nitrogen and soil/plant hydraulics. Plant, Cell Environ 19:911–927. https://doi.org/10.1111/j.1365-3040.1996.tb00456.x

Wolanin A, Rozanov VV, Dinter T, Noël S, Vountas M, Burrows JP, Bracher A (2015) Global retrieval of marine and terrestrial chlorophyll fluorescence at its red peak using hyperspectral top of atmosphere radiance measurements: Feasibility study and first results. Remote Sens Environ 166:243–261. https://doi.org/10.1016/j.rse.2015.05.018

Wutzler T, Lucas-Moffat A, Migliavacca M, Knauer J, Sickel K, Šigut L, Menzer O, Reichstein M (2018) Basic and extensible post-processing of eddy covariance flux data with REddyProc. Biogeosciences 15(16):5015–5030. https://doi.org/10.5194/bg-15-5015-2018

Xiao X, Hollinger D, Aber J, Goltz M, Davidson EA, Zhang Q, Moore B (2004) Satellite-based modeling of gross primary production in an evergreen needleleaf forest. Remote Sens Environ 89:519–534. https://doi.org/10.1016/j.rse.2003.11.008

Yan M, Tian X, Li Z, Chen E, Li C, Fan W (2016) A long-term simulation of forest carbon fluxes over the Qilian Mountains. Int J Appl Earth Obs Geoinf 52:512–526. https://doi.org/10.1016/j.jag.2016.07.009

Ye ZP, Yu Q (2008) A coupled model of stomatal conductance and photosynthesis for winter wheat. Photosynthetica 46(4):637–640. https://doi.org/10.1007/s11099-008-0110-0

Yu D, Shi P, Shao H, Zhu W, Pan Y (2009) Modelling net primary productivity of terrestrial ecosystems in East Asia based on an improved CASA ecosystem model. Int J Remote Sens 30(18):4851–4866. https://doi.org/10.1080/01431160802680552

Zarco-Tejada PJ, Morales A, Testi L, Villalobos FJ (2013) Spatio-temporal patterns of chlorophyll fluorescence and physiological and structural indices acquired from hyperspectral imagery as compared with carbon fluxes measured with eddy covariance. Remote Sens Environ 133:102–115. https://doi.org/10.1016/j.rse.2013.02.003

Zeng X, Shajkh M, Dai Y, Dickinson RE, Myneni R (2002) Coupling of the common land model to the NCAR community climate model. J Clim 15:1832–1854. https://doi.org/10.1175/1520-0442(2002)015%3c1832:COTCLM%3e2.0.CO;2

Zhang Y, Xu M, Chen H, Adams J (2009) Global pattern of NPP to GPP ratio derived from MODIS data: effects of ecosystem type, geographical location and climate. Glob Ecol Biogeogr 18:280–290. https://doi.org/10.1111/j.1466-8238.2008.00442.x

Zhang Y, Guanter L, Berry JA, Joiner J, van der Tol C, Huete A, Gitelson A, Voigt M, Köhler P (2014) Estimation of vegetation photosynthetic capacity from space-based measurements of chlorophyll fluorescence for terrestrial biosphere models. Global Change Biol 20:3727–3742. https://doi.org/10.1111/gcb.12664

Zhao M, Heinsch FA, Nemani RR, Running SW (2005) Improvements of the MODIS terrestrial gross and net primary production global data set. Remote Sens Environ 95:164–176. https://doi.org/10.1016/j.rse.2004.12.011